Centro de Investigación Científica y de Educación Superior de Ensenada, Baja California

Maestría en Ciencias en Ecología Marina

Insight into the foraging habitat and trophic position of yellowfin tuna (*Thunnus albacares*) in the Gulf of Mexico based on intrinsic isotope tracers

Tesis
para cubrir parcialmente los requisitos necesarios para obtener el grado de Maestro en Ciencias

Presenta:

Meliza Lyn Le Alvarado

Ensenada, Baja California, México
2020

Tesis defendida por

Meliza Lyn Le Alvarado

y aprobada por el siguiente Comité

Dra. Sharon Zinah Herzka Llona
Codirectora de tesis

Dra. Alfonsina Eugenia Romo Curiel
Codirectora de tesis

Miembros del comité

Dr. Oscar Sosa Nishizaki

Dr. Bodo Weber

Dr. Jorge Adrián Rosales Casián
Coordinador del Posgrado en Ecología Marina

Dra. Rufina Hernández Martínez
Directora de Estudios de Posgrado

Resumen de la tesis que presenta **Meliza Lyn Le Alvarado** como requisito parcial para la obtención del grado de Maestro en Ciencias en Ecología Marina.

Inferencias sobre el hábitat de alimentación y el nivel trófico del atún aleta amarilla (*Thunnus albacares*) en el golfo de México con base en trazadores isotópicos intrínsecos

Resumen aprobado por:

Dra. Sharon Zinah Herzka Llona Codirectora de tesis	**Dra. Alfonsina Eugenia Romo Curiel** Codirectora de tesis

El atún aleta amarilla (AAA, *Thunnus albacares*) es la segunda especie de túnidos con importancia comercial que es capturado en el Océano Atlántico. El Golfo de México (GM) es una de las dos zonas identificadas como áreas de desove del AAA en el Atlántico Oeste y sostiene la única pesquería objetivo en aguas oceánicas de la Zona Económica Exclusiva (ZEE) de México. Estudios de marcaje realizados en el norte del GM sugieren un alto grado de residencia en esta región. Sin embargo, se desconoce si los AAA capturados en aguas mexicanas son residentes del sur del GM o realizan migraciones temporales hacia el norte. Así mismo, el conocimiento sobre su ecología trófica en el sur del GM es escaso. En este estudio, para inferir las áreas de alimentación del AAA se hizo una comparación entre la composición isotópica ($\delta^{15}N_{bulk}$ y $\delta^{15}N_{Phe}$) de los tejidos de atunes, capturados en la porción sur del golfo, con una línea base isotópica sinóptica del GM. Con base en la distribución espacial de los valores de $\delta^{15}N_{bulk}$ y $\delta^{15}N_{Phe}$ del zooplancton, se identificaron dos líneas bases isotópicas: el norte del golfo y el centro-sur. A partir de un modelo de mezcla Bayesiana de dos fuentes se estimó la contribución proporcional de las dos regiones a los tejidos del AAA, infiriendo extensas áreas de alimentación. El $\delta^{15}N_{bulk}$ y $\delta^{15}N_{Phe}$ del músculo indican una mayor contribución de la línea base isotópica del norte del GM en la escala de tiempo de ~1 año. En la escala de tiempo de ~6 meses integrada por el hígado, el AAA se alimentó en mayor medida en la región centro-sur del golfo. Además, se calculó la posición trófica (PT) con base en (1) el análisis de isótopos estables (AIE) en tejidos completos (PT_{bulk}), con y sin considerar la contribución proporcional de las dos líneas base regionales, y (2) el AIE en compuestos específico de los AA canónico fuente y trófico (PT_{CSIA}; Phe y Glu, respectivamente). Las estimaciones de PT_{bulk} variaron en función de los factores de enriquecimiento trófico (FET) aplicados. Al asumir una alimentación exclusiva en el sur del GM se obtuvieron estimaciones de PT irrazonablemente altas (5.1 a 8.6), resaltando la necesidad de considerar una posible composición isotópica múltiple para estimar la PT en especies altamente migratorias como los atunes. En contraste, al considerar la contribución proporcional de las dos líneas base regionales se obtuvo una estimación más razonable de PT de 4.2. La PT_{CSIA} fue menos variable que las estimaciones derivadas de las razones isotópicas del $\delta^{15}N_{bulk}$ con un intervalo entre 3.1 y 4.3. Siendo estas dos últimas estimaciones de PT consistentes con otras reportadas para esta especie. Estos resultados muestran que los AAA capturados dentro de la ZEE mexicana se alimentan principalmente en la región norte, así como en el centro-sur del GM, siendo la alimentación del norte una componente temporal. Los resultados de este estudio tienen implicaciones potenciales para el entendimiento de los hábitos alimentarios del AAA, su estructura poblacional y patrones de migración dentro del GM.

Palabras clave: Atún aleta amarilla, aminoácidos, alimentación, isótopos estables, nitrógeno, posición trófica

Abstract of the thesis presented **Meliza Lyn Le Alvarado** as a partial requirement to obtain the Master of Science degree in Marine Ecology

Insight into the foraging habitat and trophic position of yellowfin tuna (*Thunnus albacares*) in the Gulf of Mexico based on intrinsic isotope tracers

Abstract approved by:

Dra. Sharon Zinah Herzka Llona	**Dra. Alfonsina Eugenia Romo Curiel**
Thesis co-director	Thesis co-director

Yellowfin tuna (YFT, *Thunnus albacares*) is the second-most important commercial species of tunas fished in the Atlantic Ocean. The Gulf of Mexico (GM) is one of the two western Atlantic spawning grounds and sustains the only targetted oceanic fishery in the Mexican Exclusive Economic Zone (EEZ). Tagging studies in the northern GM suggest a high degree of residency within that region. Whether YFT caught in Mexican waters in the southern-central GM also exhibit residency or migrate to the northern gulf is currently unknown. Also, little is known regarding its trophic ecology in the southern GM. The isotopic composition ($\delta^{15}N_{bulk}$ and $\delta^{15}N_{Phe}$) of YFT tissues were compared to a synoptic system-wide isotopic baseline of the GM to infer feeding areas. Based on the spatial distribution of the $\delta^{15}N_{bulk}$ and $\delta^{15}N_{Phe}$ values of zooplankton, two isotopic baselines were identified: the northern and central-southern gulf. A two-source Bayesian mixing model was used to estimate the proportional contribution of the two regions to YFT tissues, thus inferring broad feeding areas. The combined measurements on muscle tissue indicate a greater contribution of the isotopic baseline of northern GM over the time scale of about a year. Over the time scale of about ~6 months integrated by liver tissues, YFT fed to a greater extent in the central-southern gulf. Additionally, trophic position (TP) estimates were calculated based on (1) stable isotope analysis (SIA) of bulk tissues with and without considering the proportional contribution of the two regional baselines, and (2) the compound-specific SIA of the canonical source and trophic AA (Phe and Glu, respectively). TP_{bulk} estimates varied as a function of the trophic enrichment factors (TEF) applied, which is consistent with the sensitivity of TP estimates to the selection of TEFs. Unreasonably high (5.1 to 8.6) TP estimates were obtained when assuming exclusive feeding in the southern GM, highlighting the need for considering the possibility of multiple baselines when estimating TP in highly migratory species such as tunas. In contrast, a more reasonable TP estimate of 4.2 was obtained when considering the proportional contribution of two regional baselines. TP_{CSIA} were less variable that estimates derived from bulk isotope ratios, and ranged from 3.1 to 4.3. Estimates of TP based on bulk isotope ratios and two regional baselines and CSIA of AA are consistent with previous reports for this species. Taken together, these results show that the YFT caught within the Mexican EEZ feed in northern as well as the central and southern GM, and that feeding in the northern GM has a temporal component. The findings in this study have implications for the understanding of YFT feeding, population structure and migration patterns within the GM.

Keywords: compound-specific isotope analysis, amino acids, foraging ecology, nitrogen and carbon stable isotopes, trophic position, yellowfin tuna, Gulf of Mexico

Dedication

A las estrellas más brillantes del firmamento, mi nana nené y mi feli.

Acknowledgements

Le agradezco a CICESE por haberme aceptado como estudiante de maestría en el posgrado de Ecología Marina.

A CONACYT por otorgar la beca de posgrado durante mis dos años de maestría.

Esta investigación ha sido financiada por el Fondo Sectorial CONACYT-SENER-Hidrocarburos, proyecto 201441. Esta es una contribución del Consorcio de Investigación del Golfo de México (CIGoM). Reconocemos a PEMEX por promover ante el Fondo la demanda específica sobre los derrames de hidrocarburos y el medio ambiente.

La obtención de muestras fue posible gracias al proyecto CIGOM del cual se deriva el subproyecto 6: Línea de acción 2: Caracterización del uso de hábitat por grandes vertebrados (cetáceos y pelágicos mayores).

To Dra. Leticia Barbero at NOAA's Cooperative Institute for Marine and Atmospheric Studies at the University of Miami, who was Chief Scientists during the "The Gulf of Mexico Ecosystems and Carbon Cycle 2017 Cruise" (GOMECC-3) cruise during which part of the zooplankton samples were collected. Y a Jesús por obtener estas muestras.

A mi co-directora Dra. Sharon Herzka por asesorarme durante el desarrollo de tesis y sus detalladas contribuciones a este trabajo para robustecerlo enormemente, por brindarme valiosas herramientas para crecer profesionalmente desde irme de crucero hasta cursos, y sobre todo por confiar en mí y tenerme mucha paciencia.

A mi co-directora Dra. Kena Curiel, por la retroalimentación continua a este trabajo, por las enseñanzas para estructurar mis ideas tanto en el escrito como en las presentaciones, por la edición de imágenes, por los innumerables consejos académicos y personales, y por la amistad dentro y fuera del laboratorio.

Al *Doc.* Óscar Sosa, por sus valiosas aportaciones a mi trabajo de tesis, permitirme utilizar las muestras de atún disponibles para este trabajo, por ofrecerme un lugar en el laboratorio de ecología pesquera, sus correcciones a este trabajo y por su amistad.

Al Dr. Bodo Weber, por sus valiosas contribuciones, a sus cuestionamientos sobre la biogeoquímica del golfo, comentarios y correcciones a mi trabajo de tesis.

A Masao y Felipe por embarcarse para poder traer las muestras de atunes, y en especial a Zuri porque además de aventarse esos viajes por el golfo, compartió conmigo su conocimiento sobre atún aleta amarilla y por su paciencia para enseñarme a elaborar mapas.

A Óscar Hernández y Reyna Barradas porque juntos logramos procesar todas las muestras (*bolis*) de zooplancton.

A todas las personas a bordo del buque oceanográfico Justo Sierra durante el XIXIMI-06, a las personas a bordo del GOMECC-03 y a los pescadores a bordo de los buques atuneros que fueron tan amables de recibir a mis compañeros para la obtención de muestras y que se rifan en altamar para obtener este importante recurso.

A los laboratorios de ecología pesquera I y II, a Carmencita, Luz, Mily, Tere, Frida, Felipe, Emi, Zuri, Alesa, Rafa, Óscar, Masao, Salomé, Dani, Elea, Ceci, Aurorita, Brix, Laurita, Anto, Gonza, gracias a todos por su amistad y contribuciones académicas.

A mi generación de Ecología Marina, Melina, Frida, Adonis, Hugo, Valeria, Dani, Santi, Javier, Jaime, Esperanza, gracias por todos los momentos, viajes y risas, a los decapoditos, Ale, Chris y a Mary.

A los *zorris*, mi familia que tanto amo, por ustedes estoy y soy. A mis papás que siempre me han apoyado. Y a Roberto Cortes por todo su apoyo brindado durante esta difícil etapa.

A mi hermana y mi mamá, mi mayor motivación.

Un agradecimiento muy especial a mis tíos Jimmy y Edith; los biólogos que me inspiraron a estudiar ésta bella carrera.

Table of contents

List of figures

List of tables

List of abbreviations and symbology

Abbreviation	Definition
AAs	Amino acids
Bulk	The weighted average of all components within in a specific tissue
CFL	Curved furcal length
CSIA	Compound-specific stable isotope analysis
CSIA-AA	Compound-specific stable isotope analysis of amino acids
EEZ	Economic Exclusive Zone
Glu	Glutamic acid
GM	Gulf of Mexico
SCA	Stomach content analysis
SIA	Stable isotope analysis
Phe	Phenylalanine
TDF	Trophic discrimination factor
TEF	Trophic enrichment factor
TP	Trophic position
TPx	Trophic position of x. Where x can be bulk, baseline, Bayesian CSIA.
YFT	Yellowfin tuna
δ^{15}Nx	Isotopic composition of x. Where x can be bulk, CSIA, Phe, Glu, baseline
ΔX	Difference between the isotopic composition of consumer vs. diet where x can be δ^{15}N or δ^{13}C

Chapter 1. Introduction

1.1 Atlantic yellowfin tuna

Fisheries are considered one of the most critical factors impacting the population size of top predatory fish. The return to particular foraging and spawning areas often occurs seasonally, which makes populations easily subject to fisheries overexploitation (Myers & Worm, 2003; Heithaus et al., 2008). Since the beginning of industrialized exploitation, there is an estimated global loss of more than 90% of large predators due to either target fishing or their bycatch (Myers & Worm, 2003; Graves et al., 2012). During the last 50 years, the landings of global fisheries in the northern hemisphere have changed from large piscivorous fish to planktivorous fish and small invertebrates, which implies drastic changes in the structure of marine trophic food webs (Pauly et al., 1998; Myers & Worm, 2003; Olson et al., 2014).

Yellowfin tuna (YFT), *Thunnus albacares*, is a highly valuable resource that is fished worldwide. This species constitutes the second-largest tuna fishery in the world and represents a quarter of the total catch of tunas principally for the canned market (Pecoraro et al., 2017). In the Atlantic Ocean (AO), YFT is the second most important species supporting commercial and recreational fisheries, and it is currently managed as one panmictic stock by the International Commission for the Conservation of Atlantic Tunas (ICCAT, 2016). In the Gulf of Mexico (GM) and the Caribbean Sea, the fishery is carried out year-round, with a maximum catch during the summer (ICCAT, 2016). In Mexican waters, it is the only targeted oceanic fishery operating in the GM (DOF, 2015). YFT is classified as near-threatened by the International Union for Conservation of Nature (IUCN), and according to the most recent stock assessment, YFT in the AO is close to being overfished (ICCAT, 2016).

YFT are distributed in tropical and subtropical waters. This species belongs to the Scombridae family, which includes a great diversity of pelagic fishes such as tunas, bonitos, mackerels, and wahoos. As in other tunas, YFT has a distinctive morphology and physiology that distinguishes them from other teleosts. Their local endothermic capacity along with morphological adaptations for high-performance swimming allows them to adapt to and exploit a wide variety of habitats and makes them outstanding predators of the pelagic realm (Dewar & Graham, 1994; Watanabe et al., 2015). YFT are also depicted by a “fast” life history strategy, characterized by high fertility and early and rapid growth rate (Schaefer, 1998; Schaefer, 2001). In order to sustain the high energy demand needed for supporting their metabolism and high growth rate, tunas invest much of their energy in the search of food in pelagic oligotrophic habitats, where food availability is scarce (Olson & Boggs, 1986; Dickson, 1995; Pauly et al., 1998). Tunas have

evolved a generalist foraging strategy; they are opportunistic predators that feed in a wide variety and sizes of prey (i.e., exocoetids, scombrids, crustaceans, cephalopod, and gelatinous organisms; Brill & Bushnell, 1991; Vaske Jr & Castello, 1998; Vaske Jr et al., 2003; Potier et al., 2007; Duffy et al., 2017).

The habitat preferences of YFT are linked to high prey densities that occur in association with specific oceanographic features such as fronts, eddies, and steep bathymetry (i.e., continental slopes and seamounts), in which phytoplankton production is enhanced and therefore higher concentrations of prey occur (Holland et al., 1990; Nishida et al., 2001; Schaefer et al., 2007; Weng et al., 2009; Teo & Block, 2010). Habitat utilization of YFT is also greatly influenced by temperature and dissolved oxygen concentration (Schaefer et al., 2007). This species is most commonly found in warm waters above 22°C and at oxygen concentrations >3.5 ml L^{-1} (Korsmeyer et al., 1997; Brill et al., 2005). Consequently, vertical movements of YFT are restricted to the mixed layer with only occasional dives below the thermocline for short periods (Holland et al., 1990; Hoolihan et al., 2014). Although YFT is an opportunistic predator, these environmental constraints influence the feeding behavior of YFT, as they tend to feed on pelagic prey found near the warmer surface waters (Holland et al., 1990; Dambacher et al., 2010; Olson et al., 2014; Houssard et al., 2017). As in other highly migratory pelagic species, tunas serve as ecological links and a means of energy transfer between ocean basins (Block et al., 2011; Young et al., 2015; Richardson et al., 2018;). While the movement of these predators between habitats is due to shifts in key resources, such as prey availability or breeding habitat requirements, they typically spend more time foraging in habitats with higher production, often exhibiting some degree of site fidelity. Predators that occupy the highest trophic positions can integrate the energy flow of the ecosystem in which they forage (Boyd et al., 2006). Hence, the trophic position of top predators such as YFT provides an indicator of the integrity and health of the habitat where they forage.

YFT performs extensive transoceanic migrations associated with feeding and spawning. Their migration across the AO has been documented based on tag-recapture studies; individuals tagged in the GM have also been recaptured in the Gulf of Guinea, corroborating the connectivity between these regions (ICCAT, 2006; Ortiz, 2017). Four spawning areas are recognized within the AO: two in the eastern Atlantic (Cape Verde and the Gulf of Guinea), and two in the western Atlantic (the GM and the Caribbean Sea) (Richards, 1969; Arocha et al., 2001; Ortiz, 2017). In the GM the spawning season is between May and August, as indicated by the presence of spawning females and high larval abundance in the northern gulf (Lang et al., 1994; Arocha et al., 2001; Cornic et al., 2018). Recently, the natal origin of YFT captured in the northern GM has been inferred by Kitchens (2017) based on the analysis of otoliths microchemistry of

juvenile YFT ($\delta^{13}C$ and $\delta^{18}O$ analysis of carbonates and trace elements); she found that half of the adult and sub-adults inhabiting the GM originate *in situ*, while the natal origin of the rest is the eastern Atlantic.

YFT behavior and movements within the GM have been assessed by pop-up satellite archival tagging and through modeling relating ocean conditions with catch data collected by the longline fishery (Weng et al., 2009; Teo & Block, 2010; Hoolihan et al., 2014; Abad-Uribarren et al., 2019). Weng et al. (2009) briefly described their diel vertical movements from the surface to the margins of the deep scattering layer (~100 m) presumably in search of prey, but the analysis was based on only six tags, which limits inferences regarding their feeding behavior. Rooker et al. (2019) tracked the horizontal movements of > 50 individuals that were tagged with pop-up archival tags in the GM between 2008-2016 and found limited spatial displacement within the U.S. Economic Exclusive Zone (EEZ), as well as limited movements to Mexican waters during fall and winter.

This pattern was also previously noted by Hoolihan et al. (2014) based on 25 pop-up satellite tags that were deployed in a range from 14 to 95 days, with a mean displacement of ~146 km from the release to the last point and a range from 0 to 1,128 km. Hence, previous tracking studies tend to indicate prolonged residency in the northern GM. Unfortunately, long-term (> 12 months) satellite tagging data was achieved for an only limited number of individuals, thus the characterization of the full range of migratory pathways over the annual cycle may be limited. Moreover, the predominance of YFT residency in the northern gulf could represent an incomplete pattern of habitat use in the GM due to a lack of similar tagging effort in Mexican waters. Thus, the possibility of a sub-group with different movement patterns in the southern gulf cannot be eliminated. The YFT Mexican fishery registers captures year-round within the Mexican EEZ of the GM, indicating that YFT is present throughout the year in the central and southern GM and likely performing movements within the basin due to foraging and breeding requirements (DOF, 2015).

Currently, there is limited knowledge about the foraging ecology and trophic position of YFT in the southern GM. In order to assess the effects of overfishing, climate change, oil spills, and other anthropogenic and natural disturbances over the GM population of YFT, their trophic ecology must be characterized.

1.2 Stable isotope analysis and compound-specific stable isotope analysis of amino acids

Trophic position (TP) has been traditionally assessed through stomach content analysis (SCA) (i.e., Hyslop, 1980). However, SCA only allows for inferences regarding the most recently ingested diets and is labor extensive due to the need for taxonomic identification of prey sampled from the stomachs of many individuals. Movement and migration can be evaluated based on surveys of regional patterns of distribution and abundance, traditional tags, and more recently with electronic tagging or telemetry (i.e. Block et al., 2011). Traditional tagging efforts sometimes face limited success due to the low percentage of recaptured individuals, and novel satellite-based electronic tagging methods are expensive, allowing for the tagging of a limited number of individuals (Hobson et al., 2008; Young et al., 2015).

Biochemical intrinsic tracers such as stable isotopes (SIA) and compound-specific stable isotope analysis of amino acids (CSIA-AA) are complementary approaches to SCA and tagging because they provide information on diet and TP that is integrated over time and space. These characteristics are conducive to addressing questions pertaining to trophic ecology and inferring movement of marine organisms that feed in areas differing in baseline isotopic composition (Hobson, 1999; Post, 2002; Hobson et al., 2008). SIA of bulk tissues, particularly of carbon $^{13}C/^{12}C$ ($\delta^{13}C$) and nitrogen $^{15}N/^{14}N$ ($\delta^{15}N$), have been widely applied in ecological studies, including the elucidation of migratory pathways and patterns of habitat use (Peterson & Fry, 1987; Vander Zanden & Rasmussen, 1999; Post, 2002).

The $\delta^{13}C$ and $\delta^{15}N$ values reflect the isotopic composition of the assimilated diet in consumer tissues that are metabolically active (DeNiro & Epstein, 1978; Deniro & Epstein, 1981). The integration time of a tissue's isotopic composition depends on the rate of isotopic turnover, which is a function of its metabolic activity, as well as an individual's life stage and growth rate, among others, and which can be estimated empirically or through modeling (Hesslein et al., 1993; Vander Zanden & Rasmussen, 1999; Herzka, 2005).

Due to metabolic processes, isotopic discrimination against the heavy isotope occurs between a consumer and its assimilated diet, leading to tissue enrichment in ^{15}N or ^{13}C (DeNiro & Epstein, 1978; Minagawa & Wada, 1984). This isotopic discrimination is commonly reported as trophic discrimination or more recently, using the term trophic enrichment factor (TEF, Adams & Sterner, 2000; Chikaraishi et al., 2009). Because $\delta^{15}N$ values become consistently enriched in ^{15}N with each trophic level, it allows for

estimates of TP if the isotopic composition at the base of the food web (the isotopic baseline) is characterized (Peterson & Fry, 1987; Fry, 1988).

The regional biochemical process causes spatial differences in the isotopic composition of nutrient sources and primary producers, resulting in isotopic gradients (Graham et al., 2009; McMahon et al., 2013). Carbon baseline values reflect the isotopic composition of primary producers and the dissolved inorganic carbon pool (Fry & Sherr, 1989), while nitrogen depends mainly on nitrogen sources and the regionally predominant biogeochemical process (Sigman et al., 2001). The spatial distribution of isotopic values is captured in an *isoscape*, which is often constructed using the isotopic composition of primary consumers (e.g. zooplankton, benthic filter feeders; McMahon et al., 2013; Vokhshoori & McCarthy, 2014). By serving as the spatial reference of the isotopic baseline, isoscapes can be used to infer feeding habitats and movement of animals over various spatial scales (Hobson, 1999; Graham et al., 2010; McMahon et al., 2013).

If consumer $\delta^{15}N$ values are consistent with those of a local baseline, then an individual can be considered a resident that has partially or fully equilibrated to the isotopic composition of local prey, whereas recent immigrants will exhibit distinct isotopic values (Fry, 1981; Herzka, 2005; Graham et al., 2010). Although the isotopic composition of consumers has been a useful tool to estimate TP a number of requirements must be met, including a well-characterized isotopic baseline, restricted movements of the consumers within the timescale of tissue turnover rate and robust estimates of TEF (Post, 2002; Hobson & Norris, 2008). Characterizing the isotopic baseline correctly when estimating TP is crucial, because otherwise the interpretation of migration patterns, diet shifts, or both can be confounded, or the TP of the consumer can be under or over estimates (Dale et al., 2011; Seminoff et al., 2012; Madigan et al., 2014).

Recently, CSIA-AA has been developing as a complementary approach for estimating TP and inferring foraging ecology (Popp et al., 2007; Ohkouchi et al., 2017; McMahon & Newsome, 2019). The advantage of this technique is that the isotopic baseline and TP can be inferred from a single tissue sample based on isotopic analysis of a suite of amino acids (AAs; McClelland & Montoya, 2002; Chikaraishi et al., 2009). $\delta^{15}N$ values of AAs are classified based on the extent of isotopic discrimination relative to the diet. Those with little or no discrimination are the so-called *source* AAs, and those where isotopic discrimination is large are the *trophic* AAs (Popp et al., 2007). Source AAs do not readily exchange their amino-nitrogen with the metabolic pool of nitrogen, and hence do not form or break C-N bonds during transamination, resulting in very low isotope discrimination between consumers and their diet due to AA catabolism

through deamination (reviewed, O'Connell, 2017). Consequently, these AAs reflect the isotopic baseline as synthesized by primary producers and assimilated by the consumer (Figure 1). Currently, the most common source AAs used in ecology are Phenylalanine (Phe), Methionine (Met) and Lysine (Lys) (McMahon & Newsome, 2019). Since Phe has shown the lowest trophic fractionation in a diverse array of consumer-diet relationships, this AA is considered the canonical source AA and many studies have used $\delta^{15}N_{Phe}$ values to estimate $\delta^{15}N_{baseline}$ (Lorrain et al., 2009; Vokhshoori & McCarthy, 2014; McMahon & McCarthy, 2016).

On the other hand, the trophic AAs are those whose amino-nitrogen are interchangeable through transamination, thereby interacting with the metabolic pool of nitrogen, as well as being subject to deamination (O'Connell, 2017). They exhibit high N isotope discrimination between trophic levels. The trophic AAs are Glutamic Acid (Glu), Alanine (Ala), Aspartic Acid (Asp), Proline (Pro), Valine (Val), Leucine (Leu), Isoleucine (Ile) and Glutamine (Gln) (McMahon & McCarthy, 2016; O'Connell, 2017). Glutamic acid (Glu) is crucial in the metabolism of nitrogen since it is the form in which N enters the urea cycle; this AA shows high and relatively consistent isotope discrimination and has therefore been considered the canonical trophic AA (Chikaraishi et al., 2009). Based on the isotopic composition of source and trophic AAs, and empirical estimates of TEFs, the TP of the consumer can be estimated (McClelland & Montoya, 2002; Chikaraishi et al., 2009, Figure 1). Specifically, the trophic discrimination factor (TDF) is calculated as the sum of the TEFs of trophic and source AA, and used to estimate TP based on source and trophic AA measured in a single animal tissue (Popp et al., 2007; Chikaraishi et al., 2009).

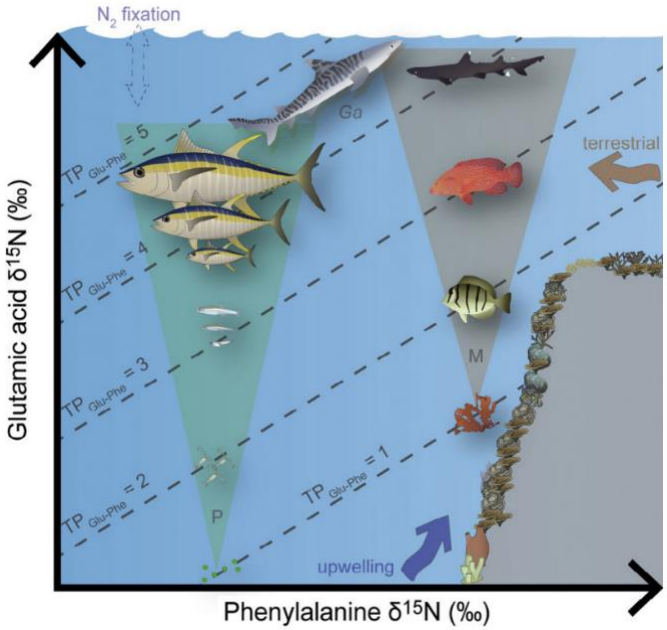

Figure 1. Schematic of two hypothetical food webs with different $\delta^{15}N$ values of Phenylalanine (Phe) and Glutamic acid (Glu). From the differences in the type of nitrogen that fuels the baseline, different habitats can be inferred. On the left side of the x-axis, an oceanic food web based on phytoplankton production (P) fueled by N_2-fixation (low $\delta^{15}N_{Phe}$ values) is depicted, and on the right side, a benthic food web based on macroalgal production (M) supported by upwelling or terrestrial run-off (high $\delta^{15}N_{Phe}$ values) is portrayed. Along the y-axis, as $\delta^{15}N_{Glu}$ values increase, so does the trophic positions of each species. Modified from Ohkouchi et al. (2017).

In the present study, intrinsic isotope tracers, specifically the carbon and nitrogen isotope ratios of bulk tissues (muscle and liver) and the canonical source AA (Phe) measured in muscle and liver tissues were used to infer the foraging habitat and TP of YFT tuna caught in southern GM. Gulf-wide zooplankton-based isoscapes were generated and regional baselines were identified within the basin. A two-source Bayesian mixing model was applied to estimate the relative contribution of each baseline to YFT tissues. Coupled with a comparison of the bulk measurements and the canonical source AA measured in tuna and zooplankton, the foraging habitat was identified. The regional baselines were also used to estimate YFT TP based on bulk SIA and CSIA.

1.3 Hypotheses

-The nitrogen and carbon isotopic composition of yellowfin tuna caught in the southern GM is consistent with the isotopic composition of the local baseline, and thus indicative of southern foraging habitat.
-Based on their feeding habits, yellowfin tuna occupies a high trophic position of 3 to 4.

1.4 Objectives

1.4.1 General objectives

Determine the foraging habitat of yellowfin tuna (*Thunnus albacares*) caught in the southern GM based on bulk stable isotope and CSIA analysis of amino acids in soft tissues (white muscle and liver) and estimate their TP.

1.4.2. Specific Objectives

-Measure the isotopic composition ($\delta^{13}C$ and $\delta^{15}N$) of bulk muscle and liver tissues, as well as the $\delta^{15}N$ values of canonical source and trophic amino acids (Phe and Glu) in white muscle and liver.
-Elaborate isoscapes for the GM based on bulk $\delta^{15}N$ values and $\delta^{15}N_{Phe}$ of zooplankton.
-Determine foraging habitat within the GM by comparing the bulk and source AA isotopic composition of yellowfin tuna versus the isotopic baseline.
-Estimate the TP of yellowfin tuna based on $\delta^{15}N$ values of bulk tissues, source and trophic amino acids using a discrete and Bayesian approach.

Chapter 2. Methods

2.1 Study area

The Gulf of Mexico (GM) is a semi-enclosed basin located in the western Atlantic (18 to 30°N, 82 to 98°W, Figure 2). One of the major drivers of mesoscale circulation is the Loop Current (LC), which penetrates the GM as the Yucatan Current trough the Yucatan Strait. The LC forms an intense anticyclonic flow that periodically extends northward toward the Mississippi River Delta or the Florida coast before exiting the basin through the Florida Straits (Molinari & Mayer, 1982). The northward penetration of the LC results in the separation of mesoscale anticyclonic eddies characterized by warm, high salinity, and oligotrophic waters that subsequently are transported westward until they dissipate (Dietrich & Lin, 1994; Sturges & Leben, 2000; Zavala-Hidalgo et al., 2006) . Occasionally, LC-eddies interact with the continental shelf and intensify coastal upwelling (Dietrich & Lin, 1994; Muller-Karger et al., 2015). The northern region of the GM (within the U.S. EEZ) is heavily influenced by the inflow of the Mississippi River system that discharges freshwater and sediment to the gulf (Milliman & Meade, 1983). Local wind stress and tidal currents provide forcing mechanisms for the mixing of freshwater and seawater, enhancing primary and secondary production in the region (Dorado et al., 2012).

In the southern GM, the Bay of Campeche is a semi-closed region (south of 22°N) that encompasses a deep water region as well as the continental shelves of the states of Veracruz, Tabasco, and Campeche, and the Campeche Bank. The bay is characterized by a semi-permanent cyclonic eddy in its southwestern reaches, and semi-permanent anticyclones in its eastern boundary near the Campeche Bank (Padilla-Pilotze, 1990; Pérez-Brunius et al., 2013). The circulation and salinity of the continental shelves (excluding the Campeche Bank) are strongly influenced by the freshwater discharge of the Grijalva-Usumacinta system (Yáñez-Arancibia et al., 2009). The Campeche Bank (or Yucatan shelf) receives nutrient-rich water throughout the year due to upwelling off Cabo Catoche, located off the northeastern Yucatan peninsula (Merino, 1997; Reyes-Mendoza et al., 2016).

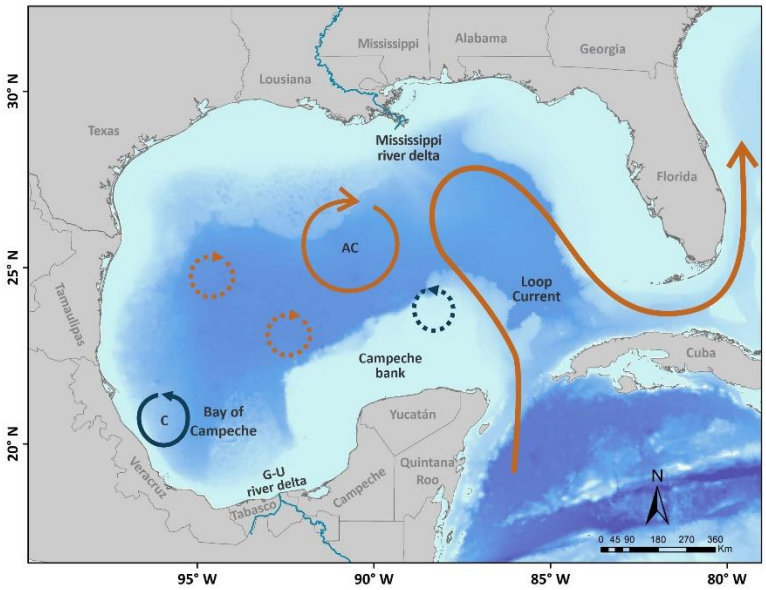

Figure 2. Schematic of the main oceanographic features that influence the circulation in the Gulf of Mexico including the Loop Current, anticyclonic eddies (AC), cyclonic eddies (C), and the Mississippi and Grijalva-Usumacinta (G-U) river deltas.

2.2 Sample Collection

During the summer of 2017 and 2018, a total of 72 yellowfin tuna samples were collected in two regions of the southern GM. The first sampling (June 12 to July 2, 2017) took place on the fishing vessel "Skypjack", and 14 tunas were captured within the Bay of Campeche (Figure 3). The second sampling period (August 7-20, 2018), was on board the fishing vessel "O-toro", and 58 tunas were sampled within the Bay of Campeche and northwest of the Yucatan platform. Both vessels are commercial longliners of the K & B Tuna S.A. of C.V. company. Longline fishing efforts used a mainline 20 to 60 km long and secondary lines (snoods) that end in "J-hooks". This fishing gear is usually used with a soaking time of 10-12 hours (Sosa-Nishizaki et al. 2017).

Captured tuna were measured for curved furcal length (CFL; cm) and a sample of white muscle (hereafter muscle) and liver of ~3 cm^3 was dissected. The muscle was extracted from the central epaxial area dorsal to the ocular cavities to preserve the integrity of tuna destined to the commercialization of high-quality fillets (Figure 4). Both tissue samples were placed in labeled plastic bags and frozen at -20°C for transport to the laboratory and subsequent isotope analysis.

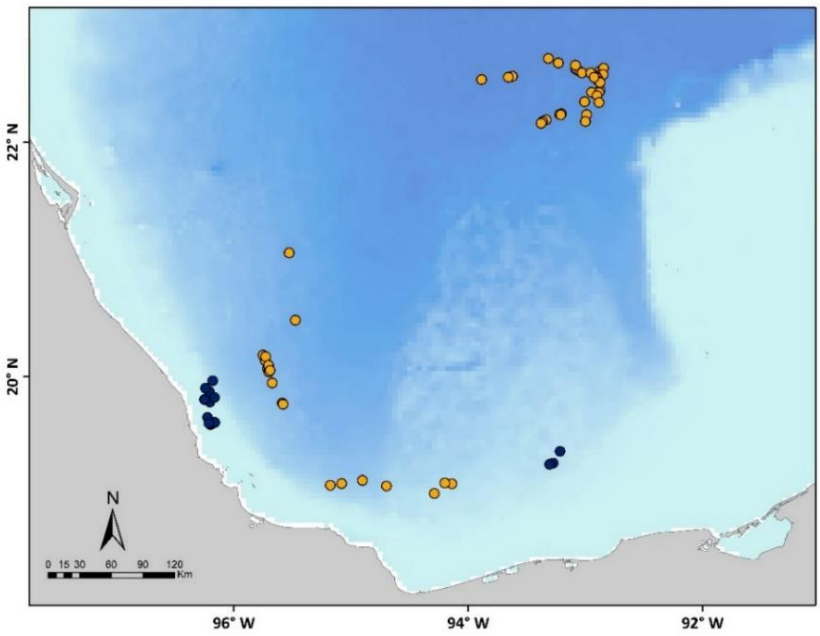

Figure 3. Sampling location of yellowfin tuna (*Thunnus albacares*) in the Bay of Campeche (dark blue dots, 2017; n=14) and in the Bay of Campeche and northwest of the Yucatan shelf (orange dots, 2018 n=58) in the Gulf of Mexico.

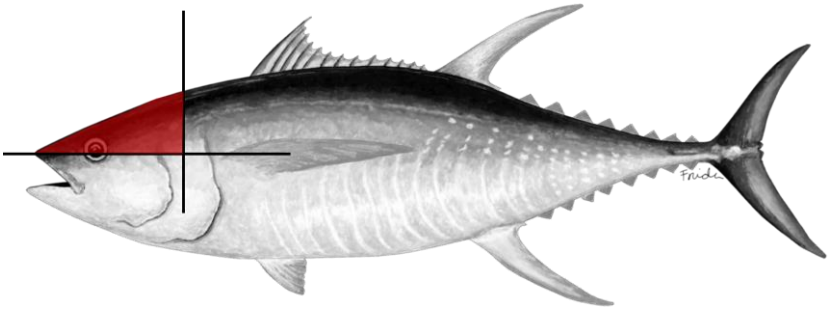

Figure 4. Location of the epaxial central region from which white muscle was dissected for bulk and amino acid analyses. Modified from CICESE® Copyright.

Samples of zooplankton were collected across the GM during two concurrent oceanographic cruises held during the summer of 2017. The XIXIMI-06 cruise was conducted by the CIGoM (Consorcio de Investigación del Golfo de México) and was held from August 18 to September 10, 2017 covering the deep water region of Mexico's EEZ (Figure 5). The Gulf of Mexico Ecosystems and Carbon Cycle 2017 Cruise (GOMECC-03) was held from July 20 to August 20, 2017 by NOAA (National Oceanic and Atmospheric

Administration). The cruise covered stations that ran along nine transects within the gulf as well as the Yucatan Channel, Florida Straits and Bahamas Channel. A total of 44 and 55 stations were covered during the XIXIMI-06 and GOMECC-03 cruises, respectively, for a total of 95 stations.

The collection of zooplankton was identical on both cruises. At each station, oblique tows to 20 m (depth permitting) were performed with 60 cm bongo nets of 4 m length and mesh size of 335 µm. The speed of cable release and recovery was 20 meters min^{-1} and a dwell time of one-minute at depth was used. Over the continental platform, tows were performed to ca. 5 m off the bottom. Of the total sample obtained from one of the nets at each station, 20% by volume was collected for zooplankton isotopic analysis by gaging to 500 ml, swirling and withdrawing two 50 ml subsamples with Hensel-Stempel pipette. Samples were frozen immediately in WhirlPack bags without preservatives.

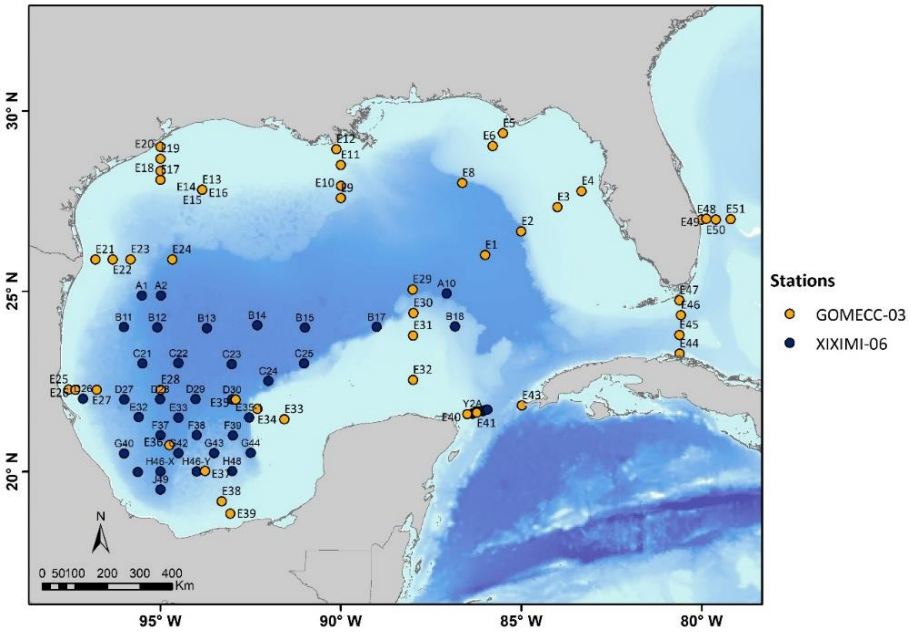

Figure 5. Location of zooplankton sampling stations in the Gulf of Mexico. Stations sampled between August 18 to September 10, 2017 during the XIXIMI-06 cruise are indicated in dark blue dots, and stations covered between July 20 and August 20 during the GOMECC-03 cruise are indicated with orange dots.

2.3 Bulk stable isotope and CSIA amino acids analyses

For bulk SIA ($\delta^{13}C$ and $\delta^{15}N$), all YFT muscle and liver tissue samples were thawed and rinsed with distilled water. From each sample, a small ~1 cm^3 portion was extracted, placed in aluminum trays and dried in a

Fisher Scientific® drying oven at 60°C for 48 hours. Dried samples were ground using an agate mortar to a fine homogeneous powder. A 0.8-1.2 mg subsample was weighed on an analytical balance, packaged in 5x9 mm Costech® tin capsules and stored in plastic trays. All utensils were cleaned with ethanol and KimWipes® to avoid contamination. Zooplankton samples were thawed and the size fraction <1000 µm and >2000 µm was separated with a sieve, dried and processed as described above.

For $\delta^{15}N$ CSIA-AA, a subset of muscle and liver tissues from 36 tunas (the entire set of samples collected in 2017 and 22 samples chose randomly from the 2018 set) and 22 samples of zooplankton >2000 µm were analyzed (Supplementary material, Tables 7, 8 and 9). Following the previously described drying and grinding method, a subsample between 7-10 mg was weighed and stored in pre-combusted 5 ml glass vials with a plastic cap. For some stations, the minimum weight required for CSIA analysis was not obtained, and samples from neighboring stations with similar bulk $\delta^{15}N$ values were combined and homogenized. All samples were stored in a desiccator prior to their analysis.

Carbon and nitrogen SIA and nitrogen CSIA-AA analysis were performed at the Stable Isotope Facility of the University of California at Davis, U.S. For SIA, samples were analyzed using a PDZ Europe ANCA-GSL elemental analyzer with an interface to a PDZ Europe 20-20 ratio mass spectrometer (Sercon Ltd., Cheshire, UK). The standard deviations (SD) of the laboratory's quality assurance materials (bovine liver, glutamic acid, enriched alanine, and Nylon 6) were 0.02‰, 0.35‰, 0.07‰, and 0.04‰, for $\delta^{15}N$ respectively, and for $\delta^{13}C$ the SD were 0.03‰, 0.10‰, 0.09‰ and 0.04‰, respectively.
Prior to CSIA-AA, samples were derivatized by esterification-acetylation (N-acetyl amino acid isopropyl esters). CSIA of individual AAs was performed on a Trace Ultra GC gas chromatograph coupled to Thermo Delta V Plus through a GC IsoLink combustion interface (Yarnes & Herszage, 2017). Each sample was analyzed in duplicate, except from samples ID 48 and 54 YFT liver and samples ID 24 and 60 YFT muscle and zooplankton station E11 (n=3) and sample ID 32 YFT muscle (n=4), for which more than two injections were used. The amino acids analyzed were Ala, Val, Glu (glutamic acid and glutamine) Ile, Leu, Pro, Asx (aspartic acid and asparagine), Phe, Lys, Met, Gly, Ser, Thr, Tyr, His, and Hyp when detectable. However, only values for the canonical source and trophic AA Phe and Glu are presented (Supplementary material, Table 7 and 8).

The standard deviation of individual AA isotope ratios from multiple (usually 2) injections of single samples for zooplankton, muscle and liver samples was generally <0.9‰. The SD of the standards used in the laboratory was generally ≤2.1 ‰, with a mean SD of 0.8‰ (Supplementary material Table 6).
The isotopic composition of the tissue and individual AAs values are reported in delta (δ) notation relative

to Vienna PeeDee Belemnite for $\delta^{13}C$ and atmospheric nitrogen for $\delta^{15}N$ (Sulzman, 2007) using the following equation (Eq. 1):

$$\delta X\ (‰) = \left[\left(\frac{R_{sample}}{R_{standard}} - 1\right)\right] \times 1000 \qquad \text{(Eq.1)}$$

where *X* is either ^{13}C or ^{15}N, and R_{sample} is the relative abundance of the heavy to light isotope ratio of the sample or standard. Isotopic values are expressed in *per mil* (‰).

2.4 Mapping of zooplankton $\delta^{15}N_{bulk}$ and $\delta^{15}N_{Phe}$ isoscapes

The first mapping of the isoscapes was based on the bulk $\delta^{15}N$ values of zooplankton < 1000 µm. The latitude and longitude of the sample locations were transformed to decimal degrees, and a Z field was generated by interpolation of the $\delta^{15}N_{bulk}$ values for each sampling station. The interpolation was performed using a non-statistical model, the IDW (Inverse Distance Weighting) method; entry values were assumed by the default functions in ArcMap, and a search distance of five times the cell size of the output raster and a power adjustment of 2 was used. To evaluate whether $\delta^{15}N_{Phe}$ values of zooplankton (fraction size of >2000 µm) reflected the bulk $\delta^{15}N$ values of zooplankton (fraction size of <1000 µm), a Pearson's linear correlation analysis was performed; there was a high correlation between bulk and $\delta^{15}N_{Phe}$ values (Pearson's correlation, $r=0.96$ $p<0.001$). A linear regression model (LRM) was used to estimate $\delta^{15}N_{Phe}$ values for stations in which direct measurements of CSIA-AA were not made to construct a second isoscape based on $\delta^{15}N_{Phe}$ values using the interpolation method previously described. The maps were constructed with the toolbox "Geostatistical Analyst" of ArcMap Version 10.3. For subsequent estimation of the contribution of baselines to YFT tissues and TP, the same isotopic baseline was assumed for both sampling years. Preliminary analysis of zooplankton isotope data from summer conditions in the southern GM for years previous to 2017 indicates interannual variability in isotope ratios was low (Hernández-Sánchez & Herzka, in prep.)

2.5 Bayesian stable isotope mixing model to estimate the proportional contribution of two baselines to yellowfin tuna tissues

Based on the spatial distribution of the zooplankton isotope composition, two baselines were considered: one for the northern GM and another for the central-southern GM baselines (see Results). To assess the relative contribution of two potential sources to YFT tissues, a Bayesian stable isotope mixing model was implemented. This model is used to estimate the contribution of prey sources to a consumer's diet while considering variability in their isotopic composition. Mean zooplankton $\delta^{13}C$ and $\delta^{15}N$ values for each baseline were corrected for their trophic enrichment factor by assuming YFT prey TP= 3.2 (one TP below YFT TP= 4.2, based on the results of this study; see Results).

Empirically derived TEFs were those reported for Pacific bluefin tuna (*Thunnus orientalis*) held in captivity: $\Delta^{13}C$= 1.8‰ and $\Delta^{15}N$= 1.9‰ for muscle and $\Delta^{13}C$= 1.2‰ and $\Delta^{15}N$= 1.1‰ for liver (Madigan et al., 2012a). Although there are TEF for YFT, these estimates are based on wild-caught juveniles (CFL ≤35 cm; Graham, 2008), that did not achieve isotopic equilibrium with the diet, a necessary prerequisite for estimating TEF. In contrast, those calculated for Pacific bluefin tuna were obtained in larger individuals 62.5-75 cm in CFL. Additionally, these TEFs were the only available estimates for muscle and liver for both elements (C and N) in tunas.

The Bayesian model was run with uninformed priors, no concentration dependence, four Markov Chain Monte Carlo (MCMC) chains, and 1000 burn-in and 10,000 iterates to calculate the posterior distribution and compute credibility intervals (Bayesian confidence intervals) (Parnell et al., 2013). Results are reported as a proportional contribution of each baseline (%) at mode 95% and [Credibility Interval]. Mixing model results were estimated with the *SIMMR* package as an upgrade to the *SIAR* package in Rstudio Version 1.1.463 –© 2009-2018 (R development Core Team 2008).

2.6 Yellowfin tuna trophic position estimates

To estimate the discrete TP of YFT based on $\delta^{15}N_{bulk}$ values of muscle and liver (hereafter refer as TP_{bulk}) Post's (2002) equation was used (Eq. 2):

$$\mathrm{TP}_x = \left(\frac{\delta^{15}N_x - \delta^{15}N_{Baseline}}{TEF}\right) + TP_{Baseline} \quad \text{(Eq. 2)}$$

Where *x* is YFT, the $\delta^{15}N_{baseline}$ corresponds to the isotopic composition of primary consumers in the region where they feed (inferred with the mixing model), and $TP_{baseline}$ is the TP of primary consumers. For this study, a $TP_{baseline}$ of 2 was used following the TP estimate for zooplankton size 200-1000 µm in the North Atlantic (Basedow et al., 2016). In calculating TP_{bulk} for YFT, we used an array of TEF values that have been applied in other studies on the same species (Table 2).

Additionally, a Bayesian approach was implemented to estimate TP_{bulk} of YFT; an advantage of this method is that the isotopic composition of two baselines and two elements (C and N) can be incorporated into TP estimates by running a simple mixing model. This allows differentiating between two distinct sources of nitrogen. $\delta^{13}C$ and $\delta^{15}N$ values of zooplankton from the northern (n=28) and central-southern (n=61) region of the GM were used as baselines. TP_{bulk} was estimated for YFT muscle by assuming a $TP_{baseline}$=2 and the TEFs for Pacific bluefin tuna muscle (Madigan et al., 2012a). The Bayesian model was run with uninformed priors, two MCMC chains, 20,000 iterates, and 2,000 samples per chain. The *tRophic Position* package (version 0.7.7; Quezada-Romegialli et al., 2018) was used in Rstudio Version 1.1.463 – © 2009-2018 (R Development Core Team 2008).

Because there were no significant differences in the $\delta^{15}N_{bulk}$ values of muscle and liver between years (one-way ANOVA, p=0.77 and p=0.70, respectively), data for both were pooled for estimating TP_{bulk}.

To estimate the TP based on nitrogen CSIA-AA (TP_{CSIA}), the equation by Chikaraishi et al. (2009) was used (Eq. 3):

$$\mathrm{TP}_{x/y} = \frac{\left(\delta^{15}N_x - \delta^{15}N_y - \beta\right)}{(TDF)} + 1 \quad \text{(Eq. 3)}$$

Where *x* is the canonical trophic AAs (Glu), *y* is the canonical source AA (Phe), and β represents the difference between the $\delta^{15}N$ values of trophic and source AAs in primary producers (β= 3.4± 0.9‰ estimate based on 17 aquatic photoautotrophs; Chikaraishi et al. 2009). This value has been used in other TP_{CSIA} estimates for YFT and Pacific bluefin tuna (Lorrain et al., 2015; Madigan et al., 2016). The trophic discrimination factor (TDF) reflects the cumulative isotope discrimination of the source and trophic AA per trophic level (Chikaraishi et al., 2009; Popp et al., 2007). Some studies suggest that TDFs values may be taxon-specific and that they may vary as a function of protein quantity and quality, as well as an organism's

TP (Hoen et al., 2014; Nielsen et al., 2015; Bradley et al., 2015; Nuche-Pascual, 2018). Hence, we calculated TP_{CSIA} using various literature-derived TDFs (Table 2) and compared the results to those obtained using bulk $\delta^{15}N$ values and the results of SCA.

2.7 Statistical analyses

Curved furcal length, $\delta^{15}N$, $\delta^{13}C$, $\delta^{15}N_{Phe}$, and $\delta^{15}N_{Glu}$ values were tested for normality by groups (year or tissue type) using the Shapiro-Wilk test. Homoscedasticity of variance was evaluated with Bartlett's test for groups exhibiting normality and with Levene's test for those that failed to show normality (the latter test is less sensitive to deviations from normality, Levene, 1960). Differences between mean CFL, $\delta^{15}N$, $\delta^{13}C$, $\delta^{15}N_{Phe}$, and $\delta^{15}N_{Glu}$ values between either years or tissues were tested using one-way ANOVA with *post hoc* Tukey's or Dunn's tests for groups with a normal distribution, and with a nonparametric Kruskal-Wallis test (KWt) with *post hoc* Mann-Whitney-U test (MWUt) when data failed to exhibit normality. The level of significance of all statistical tests used was 0.05 (α=0.05). Linear regression analyses of $\delta^{15}N$ and $\delta^{13}C$ values of muscle and liver with tuna CFL were done to evaluate whether the isotopic composition was correlated to YFT size. A linear regression analysis of zooplankton bulk $\delta^{15}N$ vs $\delta^{15}N_{Phe}$ values was done to evaluate the level of correlation between these measurements, and derive a model to estimate zooplankton $\delta^{15}N_{Phe}$ values for stations that were not analyzed. Analyses were performed with the *pgirmess* package in Rstudio Version 1.1.463 – © 2009-2018 (R Development Core Team 2008) and JASP Version 0.11.1.

Chapter 3. Results

3.1. Bulk ($\delta^{15}N$ and $\delta^{13}C$) and amino acids ($\delta^{15}N$) analyses of yellowfin tuna

There were significant differences between years in mean CFL (one-way ANOVA, p=0.009; Table 1). $\delta^{13}C$ values were more variable in muscle than in liver tissue within a single year, and $\delta^{13}C$ values exhibited a narrower range (-20.1 to -18.7‰) than $\delta^{15}N$ values (6.2 to 12.8; Figure 6; Table 1). When comparing means of the isotopic composition measured in liver tissue, there were significant differences between years for $\delta^{13}C$ values (MWUt, p<0.001) but not for $\delta^{15}N$ values (one-way ANOVA, p=0.70). For muscle tissue, there were significant differences for mean $\delta^{13}C$ values but not for $\delta^{15}N$ values. Four YFT sampled in 2018 showed bulk $\delta^{15}N$ values that were particularly enriched in ^{15}N (>11.5 ‰) in muscle tissue (Figure 7), and one YFT also showed heavier $\delta^{15}N$ values in liver (10.9 ‰; Figure 6 and 7). The mean C:N ratios were higher in liver compared to muscle (Table 1). The ratios of C:N in liver in this study were considered high with ratios >3.5 reported by Post et al. (2007) who found a strong relationship between C:N and lipid content in animals.

When comparing between tissues, there were significant differences between both mean $\delta^{13}C$ and $\delta^{15}N$ values of bulk muscle and liver (MWUt, both p<0.001). $\delta^{13}C$ and $\delta^{15}N$ values of muscle (Figure 7a) and liver (Figure 7b) correlated positively, and for both elements muscle tissue showed heavier values. There was a lack of a linear relationship between CFL and $\delta^{13}C$ values for both tissues. In contrast, there was a weak but significant correlation between CFL and $\delta^{15}N$ values for both tissues (Figure 8b).

For CSIA-AA, no significant differences were found between mean $\delta^{15}N_{Phe}$ values of muscle and liver tissues between years (one-way ANOVA p=0.28 and p=0.70 respectively; Table 1). However, there was a significant difference between $\delta^{15}N_{Glu}$ values of muscle and liver between years (MWUt, p<0.001 and one-way ANOVA, p<0.001, respectively; Figure 9). Both $\delta^{15}N_{Phe}$ and $\delta^{15}N_{Glu}$ values were heavier in muscle than in liver tissue. Isotopic data sets that did not exhibit statistical differences between years were pooled for subsequent analyses.

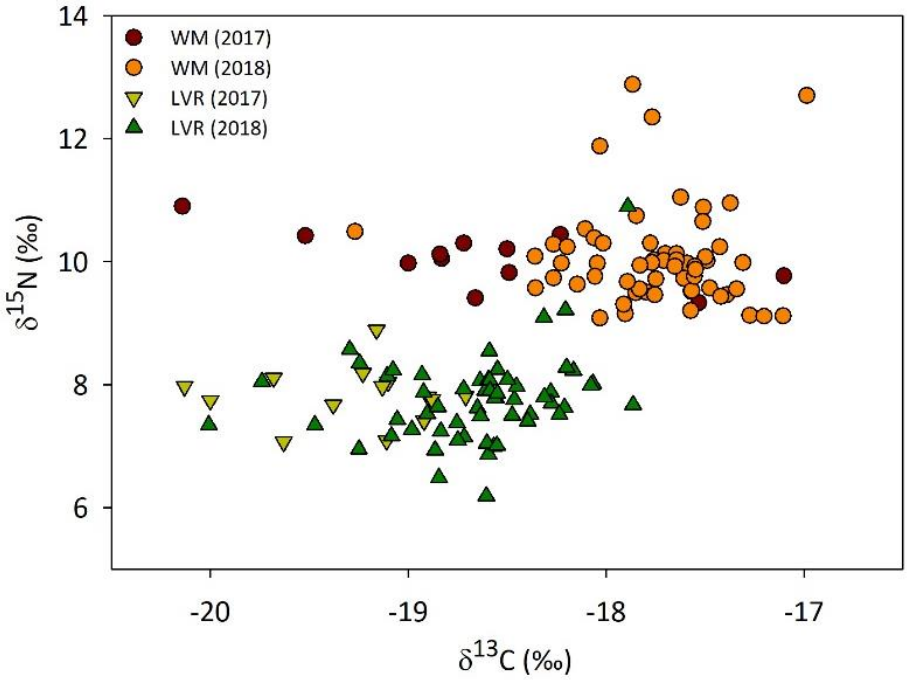

Figure 6. Scatterplot of bulk carbon vs. nitrogen isotope ratios measured in muscle (WM) and liver (LVR) tissues of 72 yellowfin tuna (*T. albacares*) caught in the southern (2017) and southern-central (2018) Gulf of Mexico.

Table 1. Number (*n*) of yellowfin tuna sampled in 2017 and 2018, curved furcal length (CFL in cm), bulk $\delta^{13}C$ and $\delta^{15}N$ values (‰), $\delta^{15}N$ (‰) values of the canonic source and trophic amino acid (AA) phenylalanine (Phe) and glutamic acid (Glu), respectively, and C:N in muscle and liver tissues. Values are means ± one standard deviation; ranges are in parenthesis.

Year	CFL (cm)	Tissue	Bulk		**$\delta^{15}N$ of canonical Source AA**	**$\delta^{15}N$ of canonical Trophic AA**	C:N
			$\delta^{13}C$ (‰)	$\delta^{15}N$ (‰)	Phe (‰)	Glu (‰)	
2017 (*n=14*)	134.9 ± 8.0 (123 to 146)**	Muscle	-18.5 ± 0.8* (-20.1 to -17.1)	10 ± 0.4 (9.3 to 10.9)	6.0 ± 1.2 (4.4 to 8.7)	26.4 ± 0.5* (25.7 to 27.1)	3.6 ± 0.4 (3.1 to 4.4)
		Liver	-19.3 ± 0.4* (-20.1 to -18.7)	7.8 ± 0.5 (7.1 to 8.9)	4.6 ± 0.6 (3.5 to 5.9)	20.2 ± 0.6*** (18.9 to 21.8)	4.1 ± 0.3 (3.8 to 4.7)
2018 (*n=58*)	140.5 ± 6.9 (128 to 160) **	Muscle	-17.8 ± 0.4* (-19.3 to -17.1)	10.1 ± 0.8 (9.1 to 12.9)	6.5 ± 1.4 (4.0 to 9.1)	25.3 ± 1.4* (23.1 to 28.6)	3.3 ± 0.2 (3.1 to 3.9)
		Liver	-18.7 ± 0.4 (-20 to -17.9)	7.8 ± 0.7 (6.2 to 10.9)	4.1 ± 1.3 (1.7 to 6.8)	19.1 ± 0.8 (17.4 to 21.4)	4.2 ± 0.3 (3.7 to 5.2)

*Indicates significant differences in the same tissue between years and differences in CFL between years tested with Kruskal-Wallis and Mann-Whitney *post hoc* tests. Significance levels are indicated as: *** for 0.001, ** for 0.001 and * for 0.01.

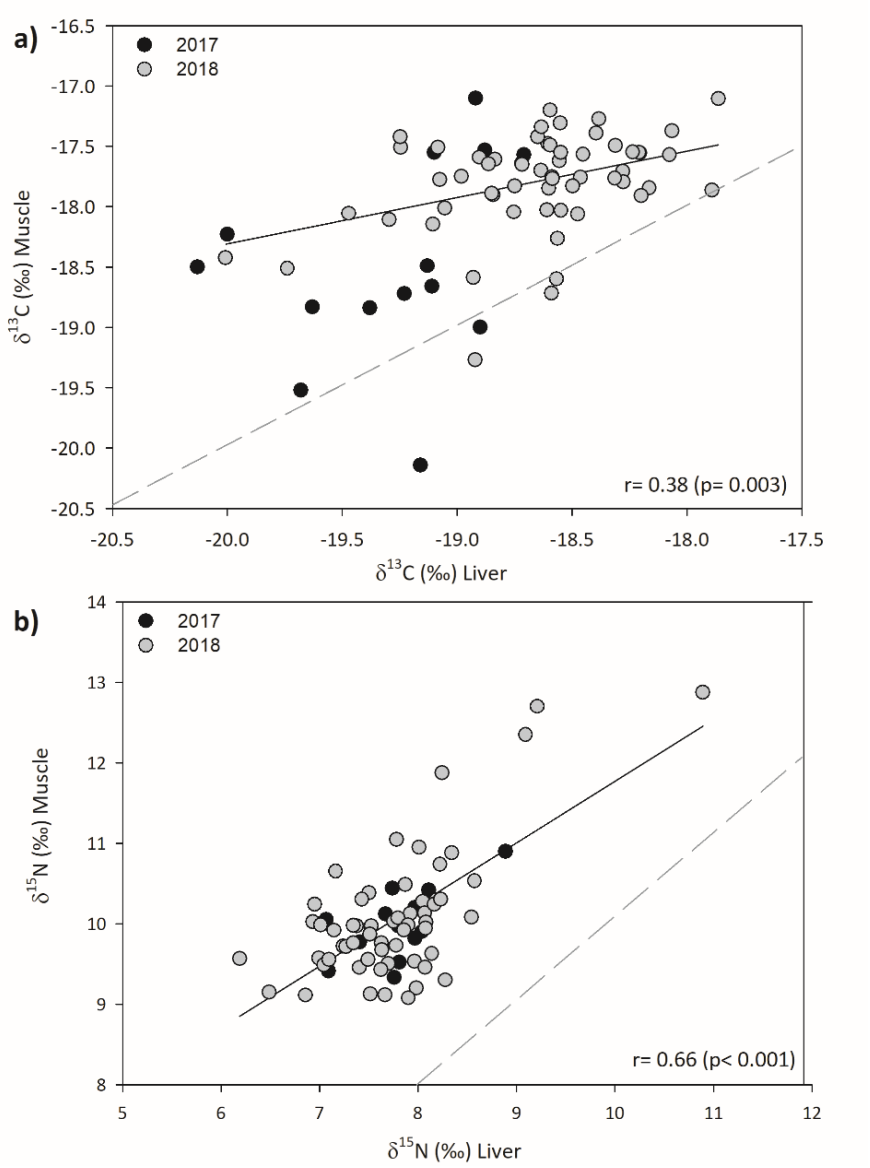

Figure 7. Linear correlation between bulk carbon (a) and nitrogen (b) isotope ratios measured in liver and muscle tissue of yellowfin tuna (*T. albacares*) collected in the southern (2017) and central (2018) Gulf of Mexico. The line in (a) corresponds to the regression line for 2018 data only; the correlation for the 2017 data was not significant. The broken line is a reference 1:1 line.

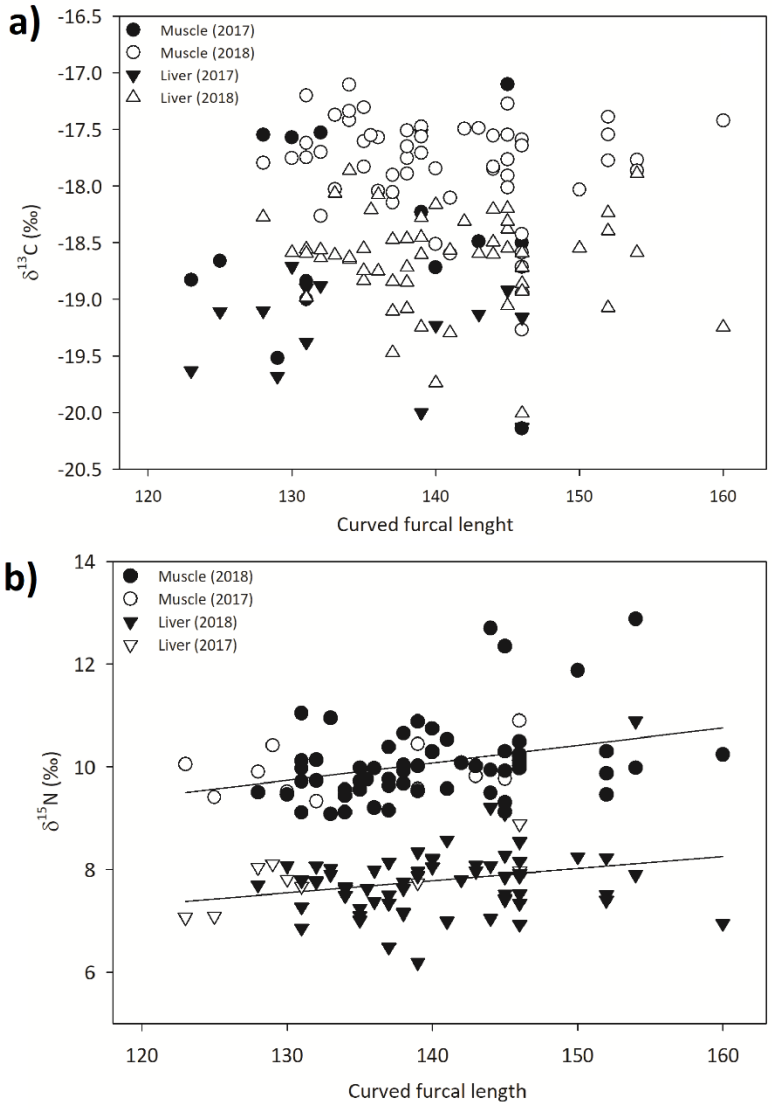

Figure 8. Yellowfin tuna curved furcal length in cm vs. bulk $\delta^{13}C$ values (a) and $\delta^{15}N$ values (b) of muscle and liver tissue. Solid lines in (b) indicate a significant linear relationship between CFL and $\delta^{15}N$ values in muscle (r= 0.34, p= 0.003) and liver (r= 0.03, p= 0.02).

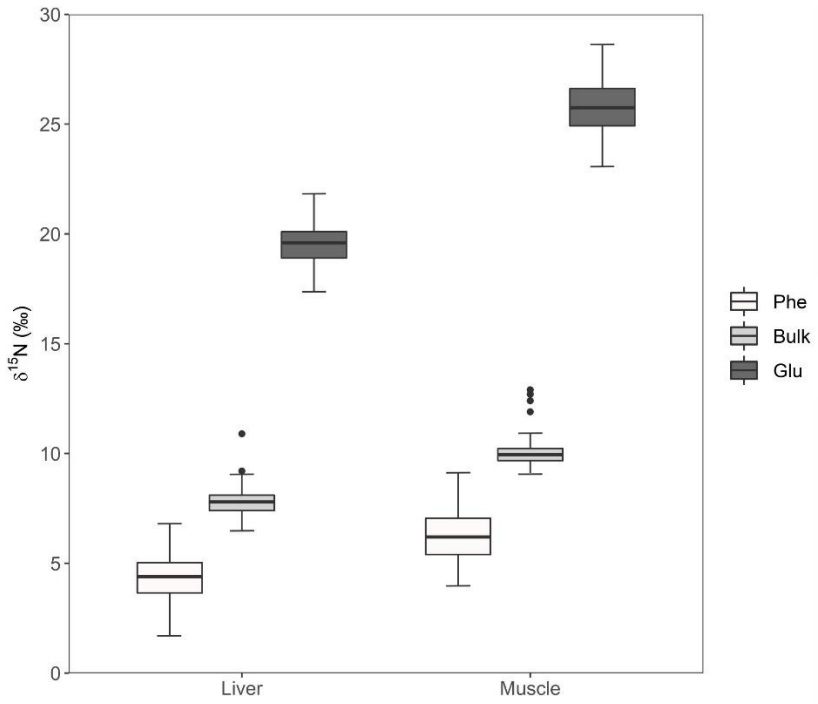

Figure 9. Comparison of $\delta^{15}N$ values of bulk tissues, phenylalanine and glutamic acid in liver and muscle tissues of yellowfin tuna (n=36) caught in 2017 (n=14) and 2018 (n=22). Boxplots display the median (bold middle line), the interquartile range (box), and the minimum and maximum observations that extend to the whiskers and outlier points beyond the whiskers.

3.2 Isoscapes and region-specific baseline values

The mean (±SD) bulk $\delta^{13}C$ values for zooplankton collected throughout the GM in 2017 was -20.3 ± 2.4‰, ranging between -21.0 to -17.3‰. However, stations sampled in the northwestern platform had zooplankton values that were relatively depleted in ^{13}C (-22.7 to -21.0‰; Supplementary material, Figure 14).

The mean bulk $\delta^{15}N$ value of zooplankton was 3.5 ± 2.2‰, and a very broad range of isotope ratios was measured (0.9 to 11.6‰). The $\delta^{15}N$ isoscape shows spatial variability, with a strong latitudinal gradient from the northern to central-southern GM (Figure 11a). Higher $\delta^{15}N$ values were observed in the coastal waters and platform off Texas, Louisiana, and Mississippi, and less enriched isotope ratios were measured in the deep-water region of the central gulf. The eastern portion of the Bay of Campeche had more enriched $\delta^{15}N$ values than the central gulf (4.5 to 6.8‰), but the isotopic composition was not as enriched in ^{15}N as those found along the coast and platform of the northern gulf.

Based on the marked north-to-south spatial gradient in baseline isotope ratios, the GM was divided into two baseline regions (the specific selection of sampling stations is indicated in Supplementary material, Table 5): the northern GM (n=28) and the central-southern GM (n=61) and mean baseline values were calculated. For the northern GM, mean $\delta^{13}C$ and $\delta^{15}N$ values for zooplankton were -21.0 ± 1.1‰ (range of averaged values was -22.7 to -19.9‰) and 6.0 ± 3.1‰ (3.1 to 11.6‰), respectively and for central-southern GM -20.2 ± 0.8 (-21.9 to -17.3) and 2.8 ± 1.0 (0.9 to 5.5), respectively.

The $\delta^{15}N_{bulk}$ and $\delta^{15}N_{Phe}$ values of zooplankton were highly correlated, although $\delta^{15}N_{Phe}$ was depleted in ^{15}N by ca. 2 ‰ relative to bulk measurements. Hence, a LRM was generated ($\delta^{15}N_{Phe} = 0.87* \delta^{15}N_{bulk} - 2.74$, Figure 10) to calculate $\delta^{15}N_{Phe}$ values for stations for which CSIA-AA measurements were not performed and used to construct the $\delta^{15}N_{Phe}$ based isoscape for the GM.

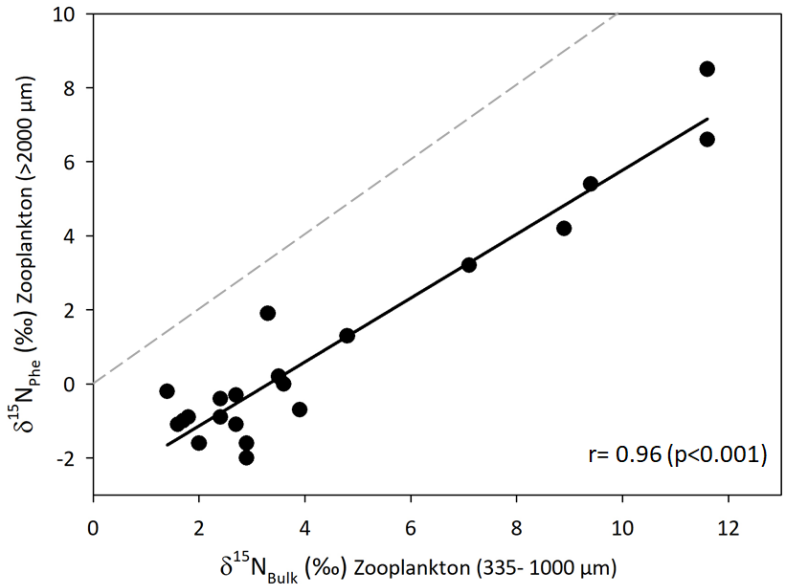

Figure 10. Linear correlation model of bulk $\delta^{15}N$ values versus $\delta^{15}N$ values of phenylalanine (Phe). The broken line is a reference 1:1 line.

Similar to those patterns observed for the $\delta^{15}N$ isoscape, the $\delta^{15}N_{Phe}$ isoscape exhibited a strong gradient from north to south (Figure 11b). Northern GM $\delta^{15}N_{Phe}$ values decrease latitudinally from 8.5‰ near the coast of Louisiana and Texas, to 3.2‰ southward, offshore of the US EEZ. In the deep water region of the GM, $\delta^{15}N_{Phe}$ values were ranged between -2.0 and 0‰, while in the southeastern Campeche Bay $\delta^{15}N_{Phe}$ values were somewhat heavier (ca. 1.9‰).

The northern GM $\delta^{15}N_{Phe}$ had a mean of 5.4 ± 2.0‰ and the central-southern GM had a mean of -0.5 ± 1.0 ‰ (based on averages of the same stations assigned to each region for the calculation of the mean bulk nitrogen isotopic baseline). Regional baselines were used for estimating the relative contribution of the bulk isotopic composition to YFT tissues, for comparing $\delta^{15}N_{Phe}$ values of regional baseline values with those of YFT tissues to show if the consumer reflects any of the baselines, and for estimating TP.

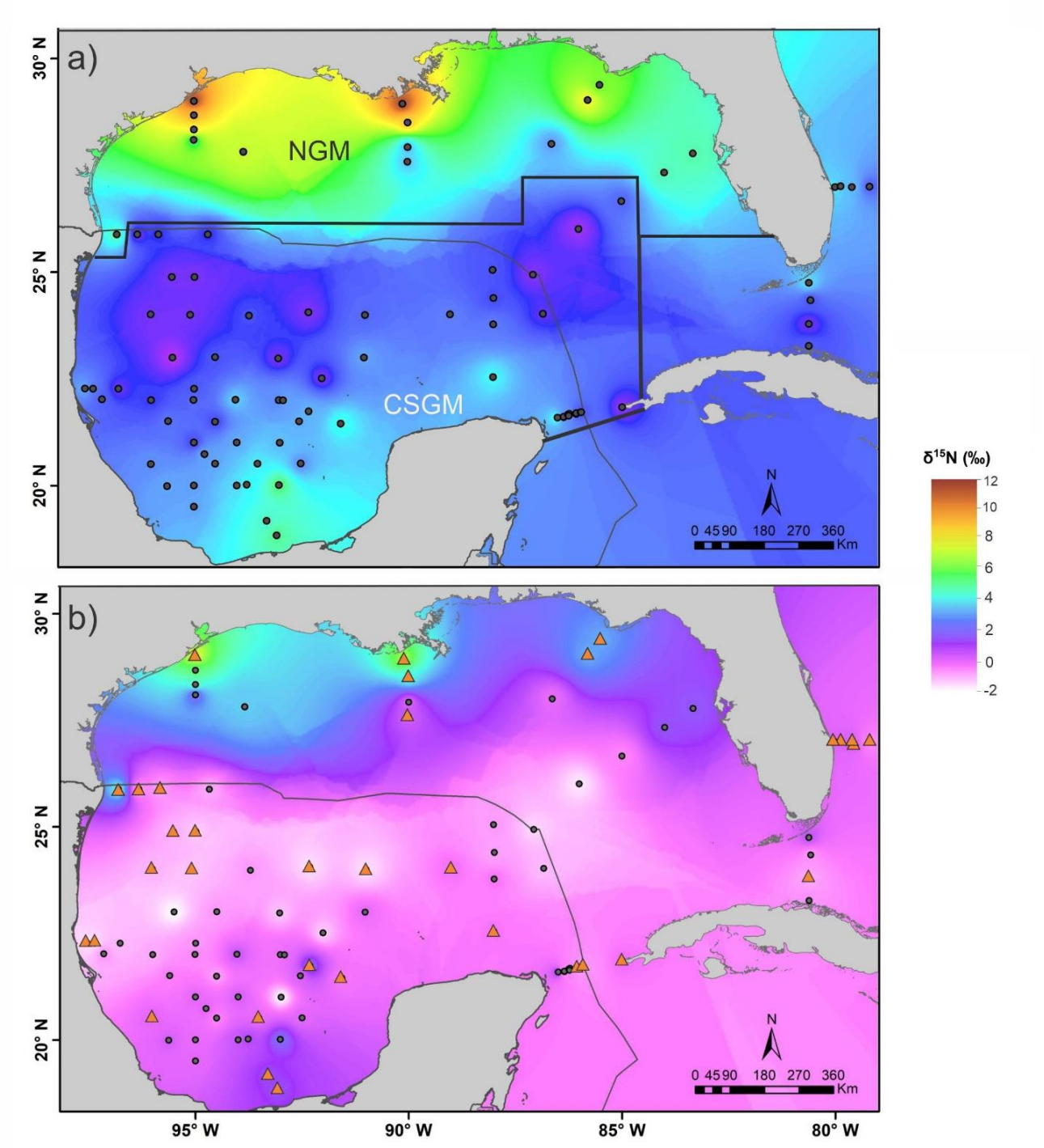

Figure 11. Gulf of Mexico (GM) zooplankton-based (a) $\delta^{15}N$ isoscape generated with IDW interpolation of 335-1000 µm zooplankton. The solid black polygon delineates the isotopic baseline regions considered for the northern (NGM) and central-southern gulf (CSGM) (b) $\delta^{15}N_{Phe}$ isoscape generated based on direct measurements of Phe in zooplankton size > 2000 µm (orange triangles) and by estimation based on a linear regression model relating $\delta^{15}N_{bulk}$ and $\delta^{15}N_{Phe}$ (grey dots). The gray line delineates the Mexican Economic Exclusive Zone.

3.3 Yellowfin tuna foraging habitat within the Gulf of Mexico

Bayesian mixing models were used to estimate the relative contribution of the TEF-corrected baselines of the northern and central-southern GM to YFT tissues. Results for muscle (estimated isotope integration time of ~334 days, Madigan et al., 2012a) indicate that the contribution of the northern GM to YFT N values was 54.9% [48.7– 62.1%], compared with 45.1% [37.9 – 51.3%] for the central-southern region. On the other hand, results for liver tissue (estimated isotope integration time of ~172 days, Madigan et al., 2012a) suggest that more recently, YFT fed to a greater extent in the central-southern GM, the contribution of the southern baseline was higher 63.7% [55.0 – 71.7%] compared with that for the northern GM of 36.3% [28.3– 45.0%] (Figure 12).

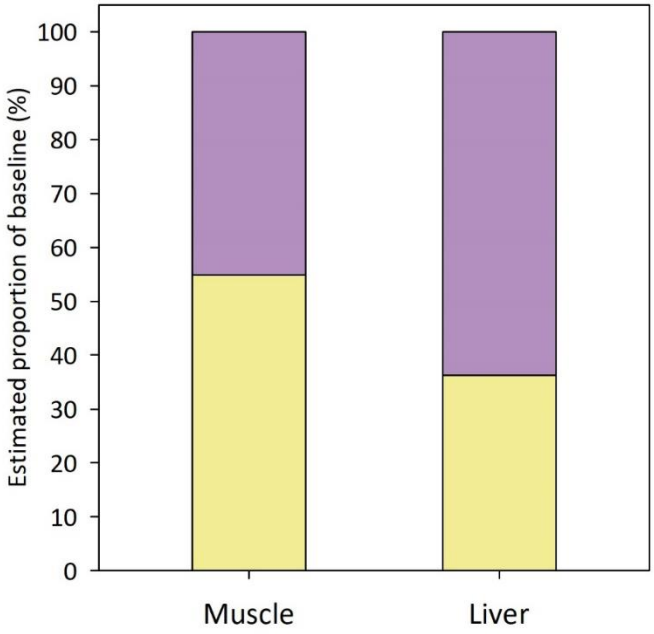

Figure 12. Isotopic baseline contributions (%) of the northern (yellow) and central-southern Gulf of Mexico to yellowfin tuna caught in the southern and central region of the GM, muscle and liver tissues based on a two-source Bayesian mixing model.

The mean $\delta^{15}N_{Phe}$ values of zooplankton collected from northern and central-southern GM baselines differed significantly (Tukey test $p<0.001$, using only data for which actual measurements were made). There were significant differences between mean YFT muscle and liver tissues and $\delta^{15}N_{Phe}$ values of central-southern GM (Tukey test, both $p<0.001$). No statistical differences were found between mean zooplankton $\delta^{15}N_{Phe}$ value of the northern GM baseline and muscle and liver tissues (Tukey test, $p= 0.25$ and $p=0.31$, respectively), suggesting the isotopic composition of the source AA in YFT tissues reflects the isotopic baseline of the northern GM.

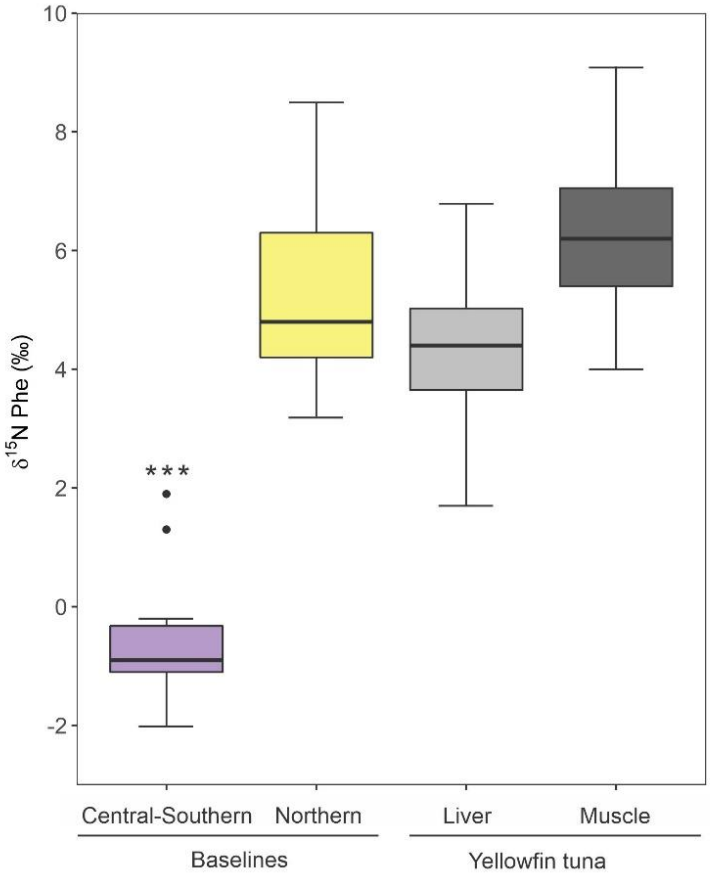

Figure 13. Comparison of $\delta^{15}N_{Phe}$ values of zooplankton collected in the central-southern and northern Gulf of Mexico (GM) and yellowfin tuna liver and muscle tissues caught in the southern and central gulf. Purple and yellow box plots represent the central-southern (n=14) and northern (n=6) Gulf of Mexico baselines, respectively. Light grey and dark grey are $\delta^{15}N_{Phe}$ values of liver and muscle of yellowfin tuna (n=36). Boxplots display the median (bold middle line), the interquartile range (box), minimum and maximum observations that extend to the whiskers and outlier points beyond the whiskers. Stars show statistical differences between $\delta^{15}N_{Phe}$ values between the central-southern GM baseline value, the northern GM baseline, and yellowfin tuna tissues based on post-hoc Tukey's tests.

3.4. Yellowfin tuna trophic position estimates

Estimates of TP_{bulk} based on muscle $\delta^{15}N$ values of YFT using five literature TEF values and using the northern GM zooplankton as a baseline ranged from 3.3 to 5.6, with a mean of 3.9 ± 0.4. Mean TP_{bulk} estimates based on liver tissue was 5.4 ± 0.7 (range 4.4 to 8.3; Table 2). In contrast, estimates of TP_{bulk} based on the central-southern GM region as baseline ranged from 4.6 to 7.3 (5.4 ± 0.5) for muscle and from 6.8 to 11.2 (8.1 ± 0.8) for liver. Overall TP_{bulk} estimates based on liver $\delta^{15}N$ values were higher and more variable than those based on muscle, and well above the TP estimates previously reported for this species by other authors (Table 3).

TP calculated with the Bayesian approach and two baselines was 4.2 [4.0 – 4.4]. This estimate is more reliable than TP_{bulk} alone using one baseline since the results of the two source contributions to YFT muscle are possible. The credibility interval is highly consistent with the global mean derived from the literature of SIA_{bulk} of 4.3 and that based on SCA of 4.0.

TP_{CSIA} estimates based on YFT muscle values ranged from 2.8 to 4.8 (3.7 ± 0.4). Applying the only TDF available for liver tissues (Nuche-Pascual et al., 2018), yielded a mean TP of 3.9 ± 0.2. Overall, TP_{CSIA} estimates (coefficient of variation, CV=11.5%) were less variables than those of TP_{bulk} (CV= 28.4%). There was a significant but low correlation between CFL and all TP_{bulk} estimates (for all TEFs applied and both tissues) with an overall $r<0.35$ (Pearson's correlation $p< 0.006$ for all cases, Supplementary material Table 10). However, there was no correlation between CFL and TP_{CSIA} (Pearson's correlation $p> 0.31$ for all correlations, Supplementary material Table 10).

Table 2. Mean trophic position (TP) estimates for yellowfin tuna caught in the central and southern Gulf of Mexico (GM) calculated with three approaches: (1) based on bulk $\delta^{15}N$ values and two regional baselines, northern GM and central-southern GM mean $\delta^{15}N$ 6.0 ± 3.1‰ and 2.8 ± 1.0‰, respectively (2) a Bayesian analysis of (bulk $\delta^{15}N$ and $\delta^{13}C$ of zooplankton and YFT tissues and two regional baselines and (3) $\delta^{15}N_{Phe}$ of YFT and zooplankton. Trophic enrichment factors (TEF) for TP_{bulk} estimates and trophic discrimination factors ($TDF = TEF_{Glu}\text{-}TEF_{Phe}$) for TP_{CSIA} estimates derived from the literature are reported in (‰).

Method	**Source**	**Organism and approach for estimations of TEFs or TDFs**	**TEF or TDF**	**Tissue**	**Calculated TP**	
					Northern GM	Central-southern GM
Bulk $\delta^{15}N$ values	Vanderklift & Ponsard (2003)	A variety of tissues in a meta-analysis of controlled studies of consumer-diet $\delta^{15}N$ enrichment factors for several taxa	2.4	Various	**3.7 ± 0.3**	**5.0 ± 0.3**
	Graham (2008)	Wild juvenile yellowfin tuna (*Thunnus albacares*)	2.1	Muscle	**3.9 ± 0.3**	**5.5 ± 0.3**
	Madigan et al. (2012a)	Pacific bluefin tuna (*Thunnus orientalis*) held in captivity	1.9	Muscle	**4.1 ± 0.4**	**5.8 ± 0.4**
	Graham (2008)	Wild juvenile yellowfin tuna (*Thunnus albacares*)	1.3	Liver	**5.1 ± 0.6**	**7.6 ± 0.6**
	Madigan et al. (2012a)	Pacific bluefin tuna held in captivity and fed with natural diet	1.1	Liver	**5.7 ± 0.7**	**8.6 ± 0.7**
Bayesian (Bulk $\delta^{15}N$ and $\delta^{13}C$)	Madigan et al. (2012a)	Pacific bluefin tuna held in captivity	$\Delta^{15}N$=1.9 $\Delta^{13}C$=1.1	Muscle	**4.2 [4.0–4.4]**	
CSIA-AA	Chikaraishi et al. (2009)	Green algae, zooplankton, and fish under cultured conditions	7.6	Muscle	**3.1 ± 0.2**	
	Bradley et al. (2014)	Pacific bluefin tuna held in captivity	6.3	Muscle	**3.5 ± 0.2**	
	Bradley et al. (2015)	Wild captures from marine teleosts combined with diet information from the literature	5.7	Muscle	**3.8 ± 0.3**	
	Nuche-Pascual et al. (2018)	Carnivorous yellowtail (*Seriola lalandi*) fed an optimal protein diet in controlled feeding experiments	4.9	Muscle	**4.3 ± 0.3**	
	Nuche-Pascual et al. (2018)	Carnivorous yellowtail fed an optimal protein diet in controlled feeding experiments	4.0	Liver	**3.9 ± 0.2**	

Table 3. Mean trophic position (TP) estimates for yellowfin tuna sampled throughout its distribution based on stomach content analysis (SCA), bulk $\delta^{15}N$ analysis, and CSIA-AA $\delta^{15}N$ of muscle tissue. The standard deviation is presented when reported by the authors or when it could be calculated from the raw data.

Reference	Location	Method	TP
Olson et al. (2010)	Pelagic eastern Pacific Ocean	SCA	3.7 ± 0.3
Bradley et al. (2015)	Eastern Tropical Pacific		4.3 ± 0.7
Pethybridge et al. (2018)	Global mean	Bulk $\delta^{15}N$	4.7 ± 0.9
Houssard et al. (2017)	Western and Central Pacific Ocean		4.3 ± 0.1
Varela et al. (2017)	Ecuadorian waters		3.7
Weng et al. (2015)	Southwestern Taiwan		4.5 ± 0.6
Logan & Lutcavage (2013)	Central North Atlantic Ocean		4.5 ± 0.3
Olson et al. (2010)	Pelagic eastern Pacific Ocean		4.7 ± 0.05
Rooker et al. (2006)	Northwestern Gulf of Mexico		3.3
Houssard et al. (2017)	Western and Central Pacific Ocean	CSIA AA $\delta^{15}N$	4.1 ± 0.7
Popp et al. (2007)	Oriental Pacific Ocean		4.4

Chapter 4. Discussion

4.1 Isotopic baselines of the Gulf of Mexico

The $\delta^{15}N_{bulk}$ and $\delta^{15}N_{Phe}$ values of zooplankton measured throughout the GM basin showed a strong geographical gradient that allowed for the separation of the basin into two regions. Specifically, the $\delta^{15}N$-based isoscape exhibited a clear latitudinal gradient, with heavy values in the north (3.1 to 11.6‰ and 3.2 to 8.5‰ for bulk and Phe, respectively) and lighter values (0.9 to 5.5‰ and -2.0 to 1.9 ‰ for bulk and Phe, respectively) in the central-southern region. The regional differences in nitrogen isotopic composition of secondary consumers (zooplankton) indicate that in order to make reliable inferences about the feeding history and TP of YFT within the GM, the $\delta^{15}N$ variability in these biogeochemical regions must be considered.

The $\delta^{15}N$ values of zooplankton samples collected near the Mississippi River plume and on the Texas and Louisiana shelves (3.3 to 8.9‰) were similar to those reported for the same group (2.6 to 7.8‰) by Dorado et al. (2012). Heavy $\delta^{15}N$ values in the northern Gulf have been associated with high inputs of freshwater discharge transporting high concentrations of dissolved nitrate from anthropogenic activities such as intensive livestock production in the central United States and inputs of treated wastewater (Rabalais et al., 2002; Bateman & Kelly, 2007). Animal manure tends to have $\delta^{15}N$ values that are enriched in ^{15}N (Szpak, 2014); manure is washed into rivers and eventually reaches coastal areas. Also, during sewage treatment, strongly discriminatory fractionation produce wastewater that is ^{15}N-enriched (Savage, 2017). Large inputs of nutrients such as nitrogen and phosphorus to coastal waters can also result in enhancement of primary and often secondary production, which in turn aggravates hypoxia and intensifies denitrification (Cloern, 2001; Rabalais et al., 2002; Rabalais et al., 2002b). This process has a large fractionation of ~25‰ (Sigman & Casciotti, 2001) that leads to a marked enrichment in the isotopic composition of ^{15}N of the inorganic nitrogen pool. The Louisiana/Texas continental shelf is one of the world's largest zones in which estuarine and coastal hypoxia has been documented (Rabalais et al., 2002). The high $\delta^{15}N$ values observed in the northern GM have been shown to reflect intense denitrification, leading to nitrate enriched in ^{15}N (Heaton, 1986; Hansson et al., 1997). A variety of processes and sources therefore contribute to the high $\delta^{15}N$ values of zooplankton in the platform and coastal areas of the northern GM, leading to a region with a distinct isotopic baseline.

In contrast to the northern GM, in the central oceanic region, very light zooplankton $\delta^{15}N$ values of 0 to 2‰ were measured. Low $\delta^{15}N$ values in phytoplankton, particulate organic matter or zooplankton have been linked to oligotrophic conditions, particularly anticyclonic eddies within the GM that are characterized by a deepening of the thermocline that limits the subsurface transport of new nitrogen (nitrate) to the surface, limiting planktonic productivity (Biggs & Ressler, 2001; Dorado et al., 2012; Wells et al., 2017). *Trichodesmium*, a diazotrophic nitrogen-fixing bacteria, is abundant in the surface waters of anticyclonic eddies and the deep water region (depths > 1000 m) of the GM (Biggs & Ressler, 2001; Holl et al., 2007). Diazotrophic bacteria are responsible for nitrogen inputs to the surface via atmospheric N_2 fixation, a process that leads to minimal isotope discrimination. Hence, fixed nitrogen has an isotopic composition of ~0‰, similar to atmospheric nitrogen (Sigman & Casciotti, 2001). These relatively light isotope ratios are reflected in the zooplankton collected in the central and southern GM.

Zooplankton from a few stations within the Bay of Campeche exhibited $\delta^{15}N$ values enriched in ^{15}N relative to the central gulf (2.9 to 5.5‰ and -0.7 to 1.3‰ for bulk and Phe, respectively). However, these isotopic values were not as high as those observed in the northern GM. These values were observed at stations located in the southwestern reaches of the bay, where the Grijalva-Usumacinta river system discharges onto the continental shelf and cross-shelf transport has been documented in late summer and early fall (Martínez-López & Zavala-Hidalgo, 2009). This region is also subject to the seasonal influence of lower temperature-high nutrient waters upwelled northeast of the Yucatan platform during spring and summer; upwelled water is transported along the shelf and slope of the Campeche Bank until it reaches the bay (Merino, 1997; Yáñez-Arancibia et al., 2009). Upwelled water has high nitrate concentration, which should have an isotopic composition similar to that reported for eastern Atlantic subsurface waters (~4.7‰; Altabet, 2006).

4.2 Yellowfin tuna foraging habitat in the Gulf of Mexico

One key aspect to making inferences about the origin and timing of previous feeding habitats of animals that move between isotopically distinct regions is to have adequate estimates of the isotopic integration time (a function of isotopic turnover rate) of the tissue of interest (Hobson, 1999). The only N isotope turnover rates for YFT were estimated based on feeding experiments with fast-growing wild-caught juveniles with mean CFL ≤ 35 cm that did not achieve isotopic equilibrium with their diet (Graham, 2008). Consequently, turnover rates were obtained through a modeling effort and were not estimated directly

The YFT sampled in this study were much larger (>123 cm CFL) than those analyzed by Graham (2008), and hence the time to equilibrium (or isotopic integration time) is likely longer than in smaller juveniles. Isotope turnover rates tend to be slower in larger fishes due to slower growth rates, and hence the fish sampled in this study would take longer to reflect a diet shift (Herzka, 2005; Vander Vander Zanden et al., 2015). In another study on a *Thunnus* (Madigan et al., 2012a), the Pacific bluefin tuna (*Thunnus orientalis*) isotope turnover rates were estimated based on feeding experiments of individuals with size at the capture of 62-75 cm. Bluefin tuna were fed with a natural diet of known isotopic composition. The experiment lasted for ~2914 days, which was sufficiently long to ensure isotopic equilibrium to the diet. Hence, the $\delta^{15}N$ turnover rate of the bluefin tuna (time to equilibrium of ~334 days and ~172 days for muscle and liver tissues, respectively) were considered more suitable estimates as a first approximation for the interpretation of the YFT analyzed in this study.

Based on the $\delta^{15}N$ values of muscle tissue, the Bayesian mixing model indicated that the northern GM baseline contributed a higher proportion (54.9%) to YFT than the southern GM (45.1%). Assuming that the isotopic composition of the baselines does not change substantially over the year, which is supported by an additional sampling of GM zooplankton (Hernández-Sánchez & Herzka, in prep.). This implies that YFT fed to a greater extent in the northern gulf. On the other hand, the more recent feeding habitat, as reflected by liver tissue with a shorter time to equilibrium (~172 days), exhibited a higher contribution of the central-southern GM baseline (63.7%). Hence, YFT had mainly fed more recently in the central-southern GM (36.3%) in which they were caught.

Given the strong correlation between zooplankton $\delta^{15}N_{bulk}$ and $\delta^{15}N_{Phe}$, the range of $\delta^{15}N_{Phe}$ values of both muscle and liver tissue also indicates the northern gulf is an important feeding habitat. As a source AA with little or no isotope discrimination (McMahon & McCarthy, 2016), $\delta^{15}N_{Phe}$ values of YFT tissues should reflect those of primary producers and secondary consumers. The $\delta^{15}N_{Phe}$ of YFT muscle (6.2 ± 1.3‰) and liver (4.1 ± 1.3‰) were not significantly different from the northern GM isotopic baseline values. However, mean liver $\delta^{15}N_{Phe}$ values were lighter (2.2‰ lower) than those of muscle tissue, which suggests more recent feeding in the central-southern GM, as calculated with the Bayesian mixing model and inferred based on the lighter bulk $\delta^{15}N$ values of liver tissue. Therefore, the coupled approaches ($\delta^{15}N$ analysis of bulk nitrogen and the source AA Phe) suggests that the main foraging ground of the YFT within the GM is the northern region, although feeding occurs in the central and southern Gulf. Unfortunately, inferences about the time-integrated could not be assessed with the source AA, since there are no published isotope turnover rates for $\delta^{15}N_{Phe}$.

The findings of this study suggest that the northern GM is an important foraging region for YFT to fulfill both biological requirements, as has been documented for other highly migratory pelagic species that use the northern GM as spawning and feeding ground (McKinney et al., 2012; Butler et al., 2015; Druon et al., 2016).Tagging studies of YFT in the northern GM show limited movements (<150 km) and a high degree of regional residency (Hoolihan et al., 2014; Rooker et al., 2019). In addition, the presence of nearly 4,000 oil rigs in the northern gulf that may serve as areas of aggregation and provide foraging opportunities that may contribute to the residency of YFT in the northern Gulf (Franks, 2000; Hoolihan et al., 2014). The northern GM also provides optimal conditions for the successful growth and survival of YFT larvae, the presence of which has been linked to high values of surface chlorophyll-a (i.e., high productivity) and intermediate salinities. These conditions are observed near the Mississippi River plume where freshwater and oceanic waters mix, and where a high abundance of YFT tuna larvae have been observed (Lang et al., 1994; Cornic et al., 2018).

Moreover, during winter, the Mexican fleet from the southern GM moves northwards toward U.S. waters, presumably "following" the abundance of YFT (Zurisaday Ramírez, Personal communication from Mexican fishermen). In a recent study by Abad-Uribarren et al. (2019) the spatial distribution of YFT monthly average CPUE was analyzed; they report a peak of relative abundance over a broad spatial range principally in the central-southern GM, and the second peak in November also across the entire study area but with higher relative abundances in the northern-central GM area further corroborating the Mexican fishermen hypothesis. This could imply that a southern sub-group of YFT may perform movements to the northern GM during winter related to feeding. However, there are no studies focusing on YFT foraging migrations relative to the distribution of their potential prey at a basin-wide scale. Elucidating the role of prey distribution on migration patterns can be challenging since YFT is a generalist predator that feeds on a wide array of prey (Vaske Jr. et al., 2003; Ménard et al., 2006; Varela et al., 2017). Nevertheless, more research is necessary to understand what drives the movement patterns within the GM, especially from the central and southern to the northern gulf. Electronic tagging in the southern GM could elucidate movement patterns and habitat use in this region.

In the temporal context of liver tissue (~6 months), my results indicate that YFT had been foraging mainly in central-southern GM. Given that the tuna in this study were caught and sampled in July and August, the feeding period reflected by liver tissue partially overlaps with the species' spawning season within the gulf (May through August). The southern GM may thus serve as an important spawning and foraging ground for YFT. However, larval surveys in the southern GM are scarce, and the morphological identification of larvae to the species level within the *Thunnus* genus is difficult or impossible (Richards,

2005). In consequence, there is limited knowledge about the larval distribution of YFT in the central and southern GM. The molecular identification (DNA barcoding) of individual larvae caught in the southern GM would further the understanding of spawning regions and patterns. Evaluation of the spatial and temporal distribution of the larvae would help determine whether this region should be reconsidered as a spawning ground.

Within the Mexican EEZ, the species supports an important fishery that operates year-round. This may be due to the high productivity of the Bay of Campeche, which is partially driven by the semi-permanent cyclone in the southwestern as well as cross-shelf transport of nutrient-rich waters (Martínez-López & Zavala-hidalgo, 2009; Pérez-Brunius et al., 2013). Cyclonic eddies upwell nutrient-rich waters that stimulate phytoplankton production that sustains a higher biomass of potential prey for top predators (Seki et al., 2001; Godø et al., 2012). The relationship of YFT to cyclonic eddies has been identified in the Indian Ocean (Tussadiah et al., 2018) and in the GM, and the higher abundance of Atlantic bluefin tuna in cyclonic eddies has also been reported (Teo & Block, 2010).

It is important to note that the interpretation of the results of this study are based on the assumption a closed population of tuna within the gulf (all tuna sampled were GM residents) and that all foraging habitats were well characterized in terms of the isotopic baseline. However, there is overlap in the bulk isotopic baselines between oceanic regions that could confound our interpretation. Similar $\delta^{15}N$ values (~3 to 8‰) to those of northern GM have been recorded in one of the YFT Eastern Atlantic spawning grounds, the Gulf of Guinea (Sandel et al., 2015). The possibility of YFT migration to the GM from the Eastern Atlantic cannot be discarded and should be evaluated using additional intrinsic tracers such as otolith microchemistry (Kitchens, 2017).

4.3 Yellowfin tuna trophic position in the Gulf of Mexico

In fish, length is positively related to TP throughout life, which is related to an individual's gape size relative to that of its prey (i.e., larger fish can feed on larger prey; McGarvey et al., 2016). Hence, the $\delta^{15}N$ values of muscle and liver tissues were examined to evaluate whether they were correlated with length. The low correlation and high variability in YFT $\delta^{15}N$ values of both tissues as a function of size are in agreement with previous reports for this species in other regions of its distribution (Ménard et al., 2007; Logan & Lutcavage, 2013; Olson et al., 2010, 2016). For example, Ménard et al. (2006) found that the size

distribution of prey in YFT stomachs was very asymmetrical, and that large YFT continue to feed on small prey during their life. This could be due to the higher availability of smaller prey relative to larger prey in the oligotrophic surface layer, were YFT spend more time (Hoolihan et al., 2014). In addition, the size range of the fish sampled in this study was small (123-160 cm CFL) which should limit the relationship between TP and size. The lack of a strong relationship between CFL and $\delta^{15}N$ values of muscle and liver tissues found in this study implies that size differences could be disregarded when estimating TP.

In this study, isotopic baselines throughout the GM were characterized and used to estimate TP. Several studies indicate that differences in the isotopic baseline between regions contribute to variation in bulk $\delta^{15}N$ values throughout the distribution of YFT (Popp et al., 2007; Graham et al., 2010; Olson et al., 2010; Lorrain et al., 2015; this study). Here, TP estimates were calculated based on (1) SIA of bulk tissues with and without considering the proportional contribution of the two regional baselines, and (2) the CSIA of the canonical source and trophic AA (Phe and Glu, respectively).

TP_{bulk} estimates using $\delta^{15}N$ values of muscle tissue and the mean isotopic composition of northern GM as baseline yielded a range of TP from 3.7 to 4.0, which is similar to that reported for other regions throughout the species' distribution (range 3.3 to 4.7; Table 3). Estimates were likely reasonable because for muscle tissue, the dominant source of N was the northern GM, and using a single baseline was an adequate first approximation to TP estimates. As has been previously noted for other regions throughout the broad distribution of YFT, bulk $\delta^{15}N$ values of muscle tissue provide robust TP estimates when the isotopic baseline is well characterized (i.e., Olson et al., 2010; Logan & Lutcavage, 2013; Weng et al., 2015; Houssard et al., 2017; Varela et al., 2017; Pethybridge et al., 2018).

The TP estimate based on the results of the Bayesian model using the $\delta^{15}N$ values of muscle yielded a more robust estimation of TP compared with the traditional TP_{bulk} estimations, in which only one baseline is taken into account. This approach performs a simple mixing model that allows for differentiation between the two sources of N, and consider for the heterogeneity caused by the different baselines (Quezada-Romegialli et al., 2018). The result was TP 4.2 [4.0–4.4], which is highly consistent with the global TP range 3.3 to 4.7 from the literature. Hence, this approach proved to provide the most realistic approximation.

In contrast, when TP_{bulk} is calculated based on muscle tissue and the mean central-southern GM isotopic composition, TP estimates are higher (5.0 to 5.8) than those calculated with the northern GM baseline. Likewise, when the central-southern GM baseline and $\delta^{15}N$ values of liver tissue are used, TP_{bulk}

are also unreasonably high and well above of YFT TP estimates reported for other regions of its distribution (TP >5.1 vs. global range from 3.3 to 4.7; see also: Logan & Lutcavage, 2013). Liver TEF values are lower and more variable than those of muscle, which contributed to the higher estimates of TPs (Madigan et al., 2012a). The lower TEF in the liver may be due to differences in its AAs composition compared with muscle, as well as its higher metabolic rate (Sweeting et al., 2005). These unreasonably high TP calculated for liver tissue suggests that $\delta^{15}N$ values of this tissue may not be a good predictor of TP.

CSIA analysis of AA eliminates the need for an independent characterization of the isotopic baseline because source AA reflect the base of the food web. TP_{CSIA} of the source and trophic AA yielded a TP range of 3.1 to 4.3. These TP are similar to those reported for YFT in other regions of its distribution based on stomach content analysis (range 3.7 to 4.3; Table 2) but were slightly lower than those estimated with $\delta^{15}N_{bulk}$ (3.3 to 5.1). The TDFs that yielded similar TP for YFT to those reported for other regions were those calculated for muscle tissue of other pelagic carnivorous teleosts (Pacific bluefin tuna and Pacific yellowtail, Bradley et al., 2014 and Nuche-Pascual et al., 2018, respectively). The widely applied TDF of 7.6‰ first proposed by Chikaraishi et al. (2009) seems to underestimate the TP of YFT (i.e., TP_{CSIA} 2.7 for the Pacific Ocean and the Indian Ocean in Lorrain et al., 2015; this study). Bradley et al. (2015) suggested that the enrichment between trophic and source AAs is lower in higher TP consumers compared with those that feed at lower trophic levels, which may be due to a higher protein consumption of carnivorous diets. In addition, TP_{CSIA} appear to underestimate the TP of taxa at or near the top of the food web; this may be due to use of empirical estimates of TDFs obtained for lower trophic level consumers or taxa that are not related taxonomically, and hence have different physiological characteristics, mode of nitrogen excretion and feeding habits (Lorrain et al., 2009; Dale et al., 2011; Germain et al., 2013; Bradley et al., 2015). In a meta-analysis of empirical estimates of TEFs available for fish muscle tissue, Nuche-Pascual et al. (submitted) found that the TEFs estimates of canonical AA were more precise when considering a single taxonomic group (teleosts). In this study, good estimates of TP_{CSIA} were obtained when using TDFs derived from lab-controlled experiments of carnivorous teleosts.

In summary, TP_{bulk} based on $\delta^{15}N$ muscle tissue values and northern GM baseline mean of 3.9 ± 0.3, as well as TP_{CSIA} considering TDFs of carnivorous teleost mean of 3.9 ± 0.3, and $TP_{Bayesian}$= 4.2[4.0-4.4] were highly consistent within the range of TP reported for YFT in other regions of its distribution based on both bulk SIA and stomach content analysis. However, TP estimates varied among individuals. This variability reflects a varied diet on prey of different trophic levels, rather than the feeding habits of a strict tertiary carnivore (commonly represented by the discrete trophic level of 4, Madigan et al., 2012b). Tunas have evolved a generalist foraging strategy, and YFT feeds on a wide variety and sizes of prey, from small

low TP pelagic crustaceans and gelatinous organisms, as well as on higher TP organisms, such as fishes and cephalopods. YFT can also feed on mesopelagic prey by occasionally expanding their vertical feeding range, although to a lesser extent than bigeye or bluefin tuna (Walli et al., 2009; Houssard et al., 2017). The YFT diet from the central North Atlantic comprises a variety of families of fishes, such as Exocoetidae, Diodontidae, Molidae, and Monacanthidae, as well as families of cephalopods including Architeuthidae, Chiroteuthidae, Histioteuthidae, Octopoda, and Ommastrephidae (Logan et al., 2013). Although SCA was not performed in this study, given the strong similarity with TP between YFT populations in other regions of its distribution, similar prey items are expected in the YFT diet within the GM.

Some research has documented shifts in YFT feeding patterns over decadal time scales, which may be due to changes in food web structure due to overfishing and/or climate change (Olson et al., 2014) . Sibert et al. (2006) analyzed the TP of exploited tunas in the Pacific Ocean and found that TP did not show an overall temporal decline over the last 60 years. In the northwestern Atlantic tuna diets and TP have remained stable for the last 50 years (Olson et al., 2016). However, a different pattern was observed for YFT in the eastern tropical Pacific during the early 1990s to 2000s, where a diet shift from larger epipelagic fish to a smaller mesopelagic species was documented over decadal time scales (Olson et al., 2014). Although past estimates of TP are unavailable for YFT in the GM, the results derived from this study provides a useful baseline for future studies on their trophic ecology.

Chapter 5. Conclusions

- Differences in nutrient sources and biogeochemical cycling on $\delta^{15}N$ values of zooplankton throughout the Gulf of Mexico basin were reflected in heavy $\delta^{15}N$ values in the neritic areas of northern GM, and lighter values in the central and southern GM. There was a strong north to south gradient for both $\delta^{15}N_{bulk}$ and $\delta^{15}N_{Phe}$ that separates the basin in two biogeochemical regions.

- The isotopic composition ($\delta^{15}N_{bulk}$ and $\delta^{15}N_{Phe}$) of muscle tissue of yellowfin tuna caught in the southern Gulf of Mexico indicated an important contribution of the food webs of the northern Gulf of Mexico, over a pre-capture foraging integrated period of about a year. The major contribution of the central-southern gulf to liver tissue is indicative of more recent feeding.

- TP_{bulk} based on $\delta^{15}N$ muscle tissue values and northern GM baseline mean of 3.9 ± 0.3, TP_{CSIA} considering TDFs of carnivorous teleost mean of 3.9 ± 0.3, and $TP_{Bayesian}$= 4.2[4.0-4.4] based on the two baseline contributions are highly consistent within the range of TP reported for yellowfin tuna in other regions of its distribution based on both bulk SIA and stomach content analysis (3.3 to 4.7) and correspond to a high TP based on feeding habits of top predators.

Cited literature

Abad-Uribarren, A., Ortega-Garcia, S., March, D., Quiroga-Brahms, C., Galvan-Magana, F., Ponce-Diaz, G. 2019. Exploring spatio-temporal patterns of the mexican longline tuna fishery in the gulf of Mexico: A comparative analysis between yellowfin and bluefin tuna distribution. Turkish Journal of Fisheries and Aquatic Sciences, 20(2), 113–125. doi:10.4194/1303-2712-v20_2_04

Adams, T. S., Sterner, R. W. 2000. The effect of dietary nitrogen content on trophic level 15 N enrichment. Limnology and Oceanography, 45(3), 601–607. doi:10.4319/lo.2000.45.3.0601chikara

Altabet, M. A. 2006. Isotopic Tracers of the Marine Nitrogen Cycle : Present and Past. En V. J.K. (Ed.), Marine Organic Matter: Biomarkers, Isotopes and DNA (Vol. 2). doi:10.1007/698_2_008

Anonymous. 2016. Report of the 2016 ICCAT yellowfin tuna stock assessment session. Collective Volume of Scientific Papers, ICCAT, 68(3), 655–817.

Arocha, F., Lee, D. W., Marcano, L. A., Marcano, J. S. 2001. Update information on the spawning of yellowfin tuna, *Thunnus albacares*, in the western central Atlantic. Collective Volume of Scientific Papers, ICCAT, 52(1), 167–176. https://www.iccat.int/Documents/CVSP/CV052_2001/n_4/CV052041395.pdf

Basedow, S. L., de Silva, N. A. L., Bode, A., van Beusekorn, J. 2016. Trophic positions of mesozooplankton across the North Atlantic: estimates derived from biovolume spectrum theories and stable isotope analyses. Journal of Plankton Research, 38, 1364–1378. doi:10.1093/plankt/fbw070

Bateman, A. S., Kelly, S. D. 2007. Fertilizer nitrogen isotope signatures. Isotopes in Environmental and Health Studies, 43(3), 237–247. doi:10.1080/10256010701550732

Biggs, D. C., Ressler, P. H. 2001. Distribution and abundance of phytoplankton, zooplankton, ichthyoplankton, and micronekton in the deepwater Gulf of Mexico. Gulf of Mexico Science, 19(1), 7–29. doi:10.18785/goms.1901.02

Block, B. A., Jonsen, I. D., Jorgensen, S. J., Winship, A. J., Shaffer, S. A., Bograd, S. J., Hazen, E. L., Foley, D. G., Breed, G. A., Harrison, A.-L., Ganong, J. E., Swithenbank, A., Castleton, M., Dewar, H., Mate, B. R., Shillinger, G. L., Schaefer, K. M., Benson, S. R., … Costa, D. P. 2011. Tracking apex marine predator movements in a dynamic ocean. Nature, 475(7354), 86–90. doi:10.1038/nature10082

Boyd, Ian L., Wanless, S., Camphuysen, C. J. 2006. Introduction. En I. L. Boyd & S. Wanless (Eds.), Top Predators in Marine Ecosystems (I). doi:10.1017/CBO9780511541964

Bradley, C. J., Madigan, D. J., Block, B. A., Popp, B. N. 2014. Amino Acid Isotope Incorporation and Enrichment Factors in Pacific Bluefin Tuna, *Thunnus orientalis*. PLoS ONE, 9(1), e85818. doi:10.1371/journal.pone.0085818

Bradley, C. J., Wallsgrove, N. J., Choy, C. A., Drazen, J. C., Hetherington, E. D., Hoen, D. K., Popp, B. N. 2015. Trophic position estimates of marine teleosts using amino acid compound specific isotopic analysis. Limnology and Oceanography: Methods, 13(9), 476–493. doi:10.1002/lom3.10041

Brill, R. W., Bigelow, K. a., Musyl, M. K. 2005. Bigeye tuna (*Thunnus obesus*) behavior and physiology and their relevance to stock assessments and fishery biology. Col. Vol. Sci. Pap. ICCAT, 57(2), 142–161. http://citeseerx.ist.psu.edu/viewdoc/download?doi=10.1.1.121.4192%7B&%7Drep=rep1%7B&%7Dtype=pdf

Brill, W., Bushnell, P. G. 1991. Metabolic and cardiac scope of high energy demand teleosts, the tunas. Canadian Journal of Zoology, 69, 2002–2009.

Butler, C. M., Logan, J. M., Provaznik, J. M., Hoffmayer, E. R., Staudinger, M. D., Quattro, J. M., Roberts, M. A., Ingram, G. W., Pollack, A. G., Lutcavage, M. E. 2015. Atlantic bluefin tuna *Thunnus thynnu*s feeding ecology in the northern Gulf of Mexico: A preliminary description of diet from the western Atlantic spawning grounds. Journal of Fish Biology, 86(1), 365–374. doi:10.1111/jfb.12556

Caut, S., Angulo, E., Courchamp, F. 2009. Variation in discrimination factors (Δ 15 N and Δ 13 C): the effect of diet isotopic values and applications for diet reconstruction. Journal of Applied Ecology, 46(2), 443–453. doi:10.1111/j.1365-2664.2009.01620.x

Chikaraishi, Y., Ogawa, N. O., Kashiyama, Y., Takano, Y., Suga, H., Tomitani, A., Miyashita, H., Kitazato, H., Ohkouchi, N. 2009. Determination of aquatic food-web structure based on compound-specific nitrogen isotopic composition of amino acids. Limnology and Oceanography: Methods, 7(11), 740–750. doi:10.4319/lom.2009.7.740

Cloern, J. 2001. Our evolving conceptual model of the coastal eutrophication problem. Marine Ecology Progress Series, 210, 223–253. doi:10.3354/meps210223

Cornic, M., Smith, B. L., Kitchens, L. L., Alvarado Bremer, J. R., Rooker, J. R. 2018. Abundance and habitat associations of tuna larvae in the surface water of the Gulf of Mexico. Hydrobiologia, 806(1), 29–46. doi:10.1007/s10750-017-3330-0

Dale, J., Wallsgrove, N., Popp, B., Holland, K. 2011. Nursery habitat use and foraging ecology of the brown stingray *Dasyatis lata* determined from stomach contents, bulk and amino acid stable isotopes. Marine Ecology Progress Series, 433(June), 221–236. doi:10.3354/meps09171

Dambacher, J. M., Young, J. W., Olson, R. J., Allain, V., Galván-Magaña, F., Lansdell, M. J., Bocanegra-Castillo, N., Alatorre-Ramírez, V., Cooper, S. P., Duffy, L. M. 2010. Analyzing pelagic food webs leading to top predators in the Pacific Ocean: A graph-theoretic approach. Progress in Oceanography, 86(1–2), 152–165. doi:10.1016/j.pocean.2010.04.011

Deniro, M. J., Epstein, S. 1981. Influence of diet on the distribution of nitrogen isotopes in animals. Geochimica et Cosmochimica Acta, 45(3), 341–351. doi:10.1016/0016-7037(81)90244-1

DeNiro, M. J., Epstein, S. 1978. Influence of diet on the distribution of carbon isotopes in animals. Geochimica et Cosmochimica Acta, 42(5), 495–506. doi:10.1016/0016-7037(78)90199-0

Dewar, H., Graham, J. B. 1994. Studies of tropical tuna swimming performance in a large water tunnel. Journal of Experimental Biology, 192, 13–31. doi:192:45-59

Dickson, K. A. 1995. Unique adaptations of the metabolic biochemistry of tunas and billfishes for life in the pelagic environment. Environmental Biology of Fishes, 42, 0–1.

Dietrich, D. E., Lin, C. A. 1994. Numerical studies of eddy shedding in the Gulf of Mexico. Journal of Geophysical Research, 99(C4), 7599. doi:10.1029/93JC03572

SECRETARIA DE AGRICULTURA, GANADERIA, DESARROLLO RURAL, PESCA Y ACUACULTURA. 2015. Plan de manejo pesquero de atún aleta amarilla (*Thunnus albacare*s) en el Golfo de México (Segunda seccion), 1–68.

Dorado, S., Rooker, J., Wissel, B., Quigg, A. 2012. Isotope baseline shifts in pelagic food webs of the Gulf of Mexico. Marine Ecology Progress Series, 464(July 2014), 37–49. doi:10.3354/meps09854

Druon, J.-N., Fromentin, J.-M., Hanke, A. R., Arrizabalaga, H., Damalas, D., Tičina, V., Quílez-Badia, G., Ramirez, K., Arregui, I., Tserpes, G., Reglero, P., Deflorio, M., Oray, I., Saadet Karakulak, F., Megalofonou, P., Ceyhan, T., Grubišić, L., MacKenzie, B. R., … Addis, P. 2016. Habitat suitability of the Atlantic bluefin tuna by size class: An ecological niche approach. Progress in Oceanography, 142(January), 30–46. doi:10.1016/j.pocean.2016.01.002

Duffy, L. M., Kuhnert, P. M., Pethybridge, H. R., Young, J. W., Olson, R. J., Logan, J. M., Goñi, N., Romanov, E., Allain, V., Staudinger, M. D., Abecassis, M., Choy, C. A., Hobday, A. J., Simier, M., Galván-Magaña, F., Potier, M., Ménard, F. 2017. Global trophic ecology of yellowfin, bigeye, and albacore tunas: Understanding predation on micronekton communities at ocean-basin scales. Deep Sea Research Part II: Topical Studies in Oceanography, 140(March), 55–73. doi:10.1016/j.dsr2.2017.03.003

Fry, B. 1981. Natural stable carbon isotope tag traces Texas shrimp migrations (*Penaeus aztecus*). Fishery Bulletin, 79(2), 337–345.

Fry, B, Sherr, E. B. 1989. δ13C Measurements as Indicators of Carbon Flow in Marine and Freshwater Ecosystems. doi:10.1007/978-1-4612-3498-2_12

Fry, B. 1988. Food web structure on Georges Bank from stable C, N, and S isotopic compositions. Limnology and Oceanography, 33(5), 1182–1190. doi:10.4319/lo.1988.33.5.1182

Germain, L., Koch, P., Harvey, J., McCarthy, M. 2013. Nitrogen isotope fractionation in amino acids from harbor seals: implications for compound-specific trophic position calculations. Marine Ecology Progress Series, 482, 265–277. doi:10.3354/meps10257

Godø, O. R., Samuelsen, A., Macaulay, G. J., Patel, R., Hjøllo, S. S., Horne, J., Kaartvedt, S., Johannessen, J. A. 2012. Mesoscale eddies are oases for higher trophic marine life. PLoS ONE, 7(1), 1–9. doi:10.1371/journal.pone.0030161

Graham, B. S, Koch, P. L., Newsome, S. D., McMahon, K. W., Aurioles, D. 2010. Using Isoscapes to Trace the Movements and Foraging Behavior of Top Predators in Oceanic Ecosystems. In J. B. West, G. J. Bowen, T. E. Dawson, & K. P. Tu (Eds.), Isoscapes (I). doi:10.1007/978-90-481-3354-3_14

Graham, B. S. 2008. Trophic dynamics and movements of tuna in the tropical Pacific Ocean inferred from stable isotope analyses. 1–126 pp.

Graham, B. S, Koch, P. L., Newsome, S. D., McMahon, K. W., Aurioles, D. 2009. Isoscapes. In Isoscapes. doi:10.1007/978-90-481-3354-3

Graves, J. E., Horodysky, A. Z., Kerstetter, D. W. 2012. Incorporating Circle Hooks Into Atlantic Pelagic Fisheries: Case Studies from the Commercial Tuna/Swordfish Longline and Recreational Billfish Fisheries. Bulletin of Marine Science, 88(3), 411–422. doi:10.5343/bms.2011.1067

Hansson, S., Hobbie, J. E., Elmgren, R., Larsson, U., Fry, B., Johansson, S. 1997. The stable nitrogen isotope ratio as marker of food-web interactions and fish migration. Ecology, 78(7), 2249–2257. doi:10.1890/0012-9658(1997)078[2249:TSNIRA]2.0.CO;2

Heaton, T. H. . 1986. Isotopic studies of nitrogen pollution in the hydrosphere and atmosphere: A review. Chemical Geology: Isotope Geoscience section, 59(C), 87–102. doi:10.1016/0168-9622(86)90059-X

Heithaus, M. R., Frid, A., Wirsing, A. J., Worm, B. 2008. Predicting ecological consequences of marine top predator declines. Trends in Ecology & Evolution, 23(4), 202–210. doi:10.1016/j.tree.2008.01.003

Herzka, S. Z. 2005. Assessing connectivity of estuarine fishes based on stable isotope ratio analysis. Estuarine, Coastal and Shelf Science, 64(1), 58–69. doi:10.1016/j.ecss.2005.02.006

Hesslein, R. H., Hallard, K. A., Ramlal, P. 1993. Replacement of Sulfur, Carbon, and Nitrogen in Tissue of Growing Broad Whitefish (*Coregonus nasus*) in Response to a Change in Diet Traced by δ34S, δ13C, and δ15N. Canadian Journal of Fisheries and Aquatic Sciences, 50(10), 2071–2076. doi:10.1139/f93-230

Hobson, K. A., Norris, R. 2008. Animal migration: A context for using new techniques and approaches. In L. I. Hobson, Keith A., Wassenaar (Ed.), Tracking animal migration with stable isotopes (2nd ed., Vol. 1). Elsevier: Saskatoon. pp. 1–20.

Hobson, K. A. 1999. Tracing origins and migration of wildlife using stable isotopes: a review. Oecologia, 120(3), 314–326. doi:10.1007/s004420050865

Hoen, D. K., Kim, S. L., Hussey, N. E., Wallsgrove, N. J., Drazen, J. C., Popp, B. N. 2014. Amino acid 15N trophic enrichment factors of four large carnivorous fishes. Journal of Experimental Marine Biology and Ecology, 453, 76–83. doi:10.1016/j.jembe.2014.01.006

Holl, C. M., Villareal, T. A., Payne, C. D., Clayton, T. D., Hart, C., Montoya, J. P. 2007. Trichodesmium in the western Gulf of Mexico: 15N2 -fixation and natural abundance stable isotopic evidence. Limnology and Oceanography, 52(5), 2249–2259. doi:10.4319/lo.2007.52.5.2249

Holland, K. N., Brill, R. W., Chang, R. K. C. 1990. Horizontal and vertical movements of yellowfin and bigeye tuna associated with fish aggregating devices. Fishery Bulletin, 88(3), 493–507.

Hoolihan, J. P., Wells, R. J. D., Luo, J., Falterman, B., Prince, E. D., Rooker, J. R. 2014. Vertical and Horizontal Movements of Yellowfin Tuna in the Gulf of Mexico. Marine and Coastal Fisheries, 6(1), 211–222. doi:10.1080/19425120.2014.935900

Houssard, P., Lorrain, A., Tremblay-Boyer, L., Allain, V., Graham, B. S., Menkes, C. E., Pethybridge, H., Couturier, L. I. E., Point, D., Leroy, B., Receveur, A., Hunt, B. P. V., Vourey, E., Bonnet, S., Rodier, M., Raimbault, P., Feunteun, E., Kuhnert, P. M., … Letourneur, Y. 2017. Trophic position increases with thermocline depth in yellowfin and bigeye tuna across the Western and Central Pacific Ocean. Progress in Oceanography, 154, 49–63. doi:10.1016/j.pocean.2017.04.008

Hussey, N. E., MacNeil, M. A., McMeans, B. C., Olin, J. A., Dudley, S. F. J., Cliff, G., Wintner, S. P., Fennessy, S. T., Fisk, A. T. 2014. Rescaling the trophic structure of marine food webs. Ecology Letters, 17(2), 239–250. doi:10.1111/ele.12226

Hyslop, E. J. 1980. Stomach contents analysis-a review of methods and their application. Journal of Fish Biology, 17(4), 411–429. doi:10.1111/j.1095-8649.1980.tb02775.x

ICCAT (International Comission for the Conservation of the Atlantic Tunas). 2006. Chapter 2.1.1: Yellowfin Tuna. In *ICCAT Manual* (pp. 27–51).

ICCAT (International Comission for the Conservation of the Atlantic Tunas). 2016. Report of the 2016 ICCAT yellowfin tuna stock assessment meeting. Col Vol Sci Pap SCRS/2016/005): 1-103

Kitchens, L. L. 2017. Origin and population connectivity of Yellowfin tuna (*Thunnus albacare*s) in the Atlantic ocean. Texas A & M. 2–5 pp.

Korsmeyer, K. E., Lai, N. C., Shadwick, R. E., Graham, J. B. 1997. Oxygen transport and cardiovascular responses to exercise in the yellowfin tuna *thunnus albacares*. The Journal of Experimental Biology, 1997, 1987–1997.

Lang, K. L., Grimes, C. B., Shaw, R. F. 1994. Variations in the age and growth of yellowfin tuna larvae,Thunnus albacares, collected about the Mississippi River plume. Environmental Biology of Fishes, 39(3), 259–270. doi:10.1007/BF00005128

Levene, Howard. 1960. "Robust tests for equality of variances". In Ingram Olkin; Harold Hotelling; et al. (eds.). Contributions to Probability and Statistics: Essays in Honor of Harold Hotelling. Stanford University Press. pp. 278–292

Logan, J. M., Lutcavage, M. E. 2013. Assessment of trophic dynamics of cephalopods and large pelagic fishes in the central North Atlantic Ocean using stable isotope analysis. Deep Sea Research Part II: Topical Studies in Oceanography, 95, 63–73. doi:10.1016/j.dsr2.2012.07.013

Lorrain, A., Graham, B. S., Ménard, F., Popp, B., Bouillon, S., van Breugel, P., Cherel, Y. 2009. Nitrogen and carbon isotope values of individual amino acids: a tool to study foraging ecology of penguins in the Southern Ocean. Marine Ecology Progress Series, 391, 293–306. doi:10.3354/meps08215

Lorrain, A., Graham, B. S., Popp, B. N., Allain, V., Olson, R. J., Hunt, B. P. V., Potier, M., Fry, B., Galván-Magaña, F., Menkes, C. E. R., Kaehler, S., Ménard, F. 2015. Nitrogen isotopic baselines and implications for estimating foraging habitat and trophic position of yellowfin tuna in the Indian and Pacific Oceans. Deep Sea Research Part II: Topical Studies in Oceanography, 113, 188–198. doi:10.1016/j.dsr2.2014.02.003

Madigan, D. J., Baumann, Z., Carlisle, A. B., Hoen, D. K., Popp, B. N., Dewar, H., Snodgrass, O. E., Block, B. A., Fisher, N. S. 2014. Reconstructing transoceanic migration patterns of Pacific bluefin tuna using a chemical tracer toolbox. Ecology, 95(6), 1674–1683. doi:10.1890/13-1467.1

Madigan, D. J., Carlisle, A. B., Dewar, H., Snodgrass, O. E., Litvin, S. Y., Micheli, F., Block, B. A. 2012. Stable Isotope Analysis Challenges Wasp-Waist Food Web Assumptions in an Upwelling Pelagic Ecosystem. Scientific Reports, 2, 1–10. doi:10.1038/srep00654

Madigan, D. J., Litvin, S. Y., Popp, B. N., Carlisle, A. B., Farwell, C. J., Block, B. A. 2012. Tissue Turnover Rates and Isotopic Trophic Discrimination Factors in the Endothermic Teleost, Pacific Bluefin Tuna (*Thunnus orientalis*). PLoS ONE, 7(11), e49220. doi:10.1371/journal.pone.0049220

Madigan, D.J., Chiang, W., Wallsgrove, N., Popp, B., Kitagawa, T., Choy, C., Tallmon, J., Ahmed, N., Fisher, N., Sun, C. 2016. Intrinsic tracers reveal recent foraging ecology of giant Pacific bluefin tuna at their primary spawning grounds. Marine Ecology Progress Series, 553(July), 253–266. doi:10.3354/meps11782

Martínez-López, B., Zavala-Hidalgo, J. 2009. Seasonal and interannual variability of cross-shelf transports of chlorophyll in the Gulf of Mexico. Journal of Marine Systems, 77(1–2), 1–20. doi:10.1016/j.jmarsys.2008.10.002

McClelland, J. W., Montoya, J. P. 2002. Trophic Relationships and the Nitrogen Isotopic Composition of Amino Acids in Plankton. Ecology, 83(8), 2173. doi:10.2307/3072049

McGarvey, R., Dowling, N., Cohen, J. E. 2016. Longer Food Chains in Pelagic Ecosystems: Trophic Energetics of Animal Body Size and Metabolic Efficiency. En The American Naturalist (Vol. 188). doi:10.1086/686880

McKinney, J., Hoffmayer, E., Wu, W., Fulford, R., Hendon, J. 2012. Feeding habitat of the whale shark *Rhincodon typus* in the northern Gulf of Mexico determined using species distribution modelling. Marine Ecology Progress Series, 458(July), 199–211. doi:10.3354/meps09777

McMahon, K. W., Hamady, L. L., Thorrold, S. R. 2013. A review of ecogeochemistry approaches to estimating movements of marine animals. Limnology and Oceanography, 58(2), 697–714. doi:10.4319/lo.2013.58.2.0697

McMahon, K. W., McCarthy, M. D. 2016. Embracing variability in amino acid δ15N fractionation: mechanisms, implications, and applications for trophic ecology. Ecosphere, 7(12), e01511. doi:10.1002/ecs2.1511

McMahon, K. W., Newsome, S. D. 2019. Amino Acid Isotope Analysis. In Tracking Animal Migration with Stable Isotopes. doi:10.1016/B978-0-12-814723-8.00007-6

Ménard, F., Labrune, C., Shin, Y., Asine, A., Bard, F. 2006. Opportunistic predation in tuna: a size-based approach. Marine Ecology Progress Series, 323(Rancurel 1976), 223–231. doi:10.3354/meps323223

Ménard, F., Lorrain, A., Potier, M., Marsac, F. 2007. Isotopic evidence of distinct feeding ecologies and movement patterns in two migratory predators (yellowfin tuna and swordfish) of the western Indian Ocean. Marine Biology, 153(2), 141–152. doi:10.1007/s00227-007-0789-7

Merino, M. 1997. Upwelling on the Yucatan Shelf: hydrographic evidence. Journal of Marine Systems, 13(1–4), 101–121. doi:10.1016/S0924-7963(96)00123-6

Milliman, J. D., Meade, R. H. 1983. World-Wide Delivery of River Sediment to the Oceans. The Journal of Geology, 91(1), 1–21. doi:10.1086/628741

Minagawa, M., Wada, E. 1984. Stepwise enrichment of 15N along food chains: Further evidence and the relation between δ15N and animal age. Geochimica et Cosmochimica Acta, 48(5), 1135–1140. doi:10.1016/0016-7037(84)90204-7

Molinari, R. L., Mayer, D. A. 1982. Current Meter Observations on the Continental Slope at Two Sites in the Eastern Gulf of Mexico. Journal of Physical Oceanography, 12(12), 1480–1492. doi:10.1175/1520-0485(1982)012<1480:CMOOTC>2.0.CO;2

Muller-Karger, F. E., Smith, J. P., Werner, S., Chen, R., Roffer, M., Liu, Y., Muhling, B., Lindo-Atichati, D., Lamkin, J., Cerdeira-Estrada, S., Enfield, D. B. 2015. Natural variability of surface oceanographic conditions in the offshore Gulf of Mexico. Progress in Oceanography, 134, 54–76. doi:10.1016/j.pocean.2014.12.007

Myers, R. A., Worm, B. 2003. Rapid worldwide depletion of predatory fish communities. Nature, 423(6937), 280–283. doi:10.1038/nature01610

Nielsen, J. M., Popp, B. N., Winder, M. 2015. Meta-analysis of amino acid stable nitrogen isotope ratios for estimating trophic position in marine organisms. Oecologia, 178(3), 631–642. doi:10.1007/s00442-015-3305-7

Nishida, T., Mohri, M., Itoh, K., Nakagome, J. 2001. Study of bathymetry effects on the nominal hooking rates of yellowfin tuna (*Thunnus albacares*) and bigeye tuna (*Thunnus obesus*) exploited by the Japanese tuna longline fisheries in the Indian Ocean. En IOTC Proceedings, 2001, 4(4), pp. 191–206. from http://wwe.iotc.org/sites/default/files/documents/proceedings/2001/wpm/IOTC-2001-WPM-02.pdf

Nuche-Pascual, M. T. 2018. Variation in bulk and amino acid-specific nitrogen isotope enrichment factors in fishes. Centro de Investigación Científica y de Educación Superior de Ensenada, Baja California.

Nuche-Pascual, M. T., Lazo, J. P., Ruiz-Cooley, R. I., Herzka, S. Z. 2018. Amino acid-specific δ15N trophic enrichment factors in fish fed with formulated diets varying in protein quantity and quality. Ecology and Evolution, 8(18), 9192–9217. doi:10.1002/ece3.4295

O'Connell, T. C. 2017. 'Trophic' and 'source' amino acids in trophic estimation: a likely metabolic explanation. Oecologia, 184(2), 317–326. doi:10.1007/s00442-017-3881-9

Ohkouchi, N., Chikaraishi, Y., Close, H. G., Fry, B., Larsen, T., Madigan, D. J., McCarthy, M. D., McMahon, K. W., Nagata, T., Naito, Y. I., Ogawa, N. O., Popp, B. N., Steffan, S., Takano, Y., Tayasu, I., Wyatt, A. S. J., Yamaguchi, Y. T., Yokoyama, Y. 2017. Advances in the application of amino acid nitrogen isotopic analysis in ecological and biogeochemical studies. Organic Geochemistry, 113, 150–174. doi:10.1016/j.orggeochem.2017.07.009

Olson, R. J, Duffy, L., Kuhnert, P., Galván-Magaña, F., Bocanegra-Castillo, N., Alatorre-Ramírez, V. 2014. Decadal diet shift in yellowfin tuna *Thunnus albacares* suggests broad-scale food web changes in the eastern tropical Pacific Ocean. Marine Ecology Progress Series, 497, 157–178. doi:10.3354/meps10609

Olson, R. J., Boggs, C. H. 1986. Apex Predation by Yellowfin Tuna (*Thunnus albacares*): independent estimates from gastric evacuation and stomach contents, bioenergetics, and cesium concentrations. Canadian Journal of Fisheries and Aquatic Sciences, 43, 1760–1775.

Olson, R. J., Popp, B. N., Graham, B. S., López-Ibarra, G. A., Galván-Magaña, F., Lennert-Cody, C. E., Bocanegra-Castillo, N., Wallsgrove, N. J., Gier, E., Alatorre-Ramírez, V., Ballance, L. T., Fry, B. 2010. Food-web inferences of stable isotope spatial patterns in copepods and yellowfin tuna in the pelagic eastern Pacific Ocean. Progress in Oceanography, 86(1–2), 124–138. doi:10.1016/j.pocean.2010.04.026

Olson, R. J., Young, J. W., Ménard, F., Potier, M., Allain, V., Goñi, N., Logan, J. M., Galván-Magaña, F. 2016. Bioenergetics, Trophic Ecology, and Niche Separation of Tunas. En Advances in marine biology. Volume 35 (Vol. 74). doi:10.1016/bs.amb.2016.06.002

Ortiz, M. 2017. Review and Analyses of Tag Releases and Recaptures of Yellowfin Tuna Iccat Db. En Collective Volume of Scientific Papers, ICCAT (Vol. 73). https://www.iccat.int/Documents/CVSP/CV073_2017/n_1/CV073010228.pdf

Padilla-Pilotze, A. R. 1990. Evidence Of A Cyclonic Eddy In The Bay Of Campeche. Ciencias Marinas, 16(3), 1–14. doi:10.7773/cm.v16i3.703

Parnell, A. C., Phillips, D. L., Bearhop, S., Semmens, B. X., Ward, E. J., Moore, J. W., Jackson, A. L., Grey, J., Kelly, D. J., Inger, R. 2013. Bayesian stable isotope mixing models. Environmetrics, (June), n/a-n/a. doi:10.1002/env.2221

Pauly, D., Christensen, V., Dalsgaard, J., Froese, R., Torres, F. 1998. Fishing Down Marine Food Webs. Science, 279(5352), 860–863. doi:10.1126/science.279.5352.860

Pecoraro, C., Zudaire, I., Bodin, N., Murua, H., Taconet, P., Díaz-Jaimes, P., Cariani, A., Tinti, F., Chassot, E. 2017. Putting all the pieces together: integrating current knowledge of the biology, ecology, fisheries status, stock structure and management of yellowfin tuna (*Thunnus albacares*). Reviews in Fish Biology and Fisheries, 27(4), 811–841. doi:10.1007/s11160-016-9460-z

Pérez-Brunius, P., García-Carrillo, P., Dubranna, J., Sheinbaum, J., Candela, J. 2013. Direct observations of the upper layer circulation in the southern Gulf of Mexico. Deep Sea Research Part II: Topical Studies in Oceanography, 85(January), 182–194. doi:10.1016/j.dsr2.2012.07.020

Peterson, B. J., Fry, B. 1987. Stable Isotopes in Ecosystem Studies. Annual Review of Ecology and Systematics, 18(1), 293–320. doi:10.1146/annurev.es.18.110187.001453

Pethybridge, H., Choy, C. A., Logan, J. M., Allain, V., Lorrain, A., Bodin, N., Somes, C. J., Young, J., Ménard, F., Langlais, C., Duffy, L., Hobday, A. J., Kuhnert, P., Fry, B., Menkes, C., Olson, R. J. 2018. A global meta-analysis of marine predator nitrogen stable isotopes: Relationships between trophic structure and environmental conditions. Global Ecology and Biogeography, 27(9), 1043–1055. doi:10.1111/geb.12763

Popp, B. N., Graham, B. S., Olson, R. J., Hannides, C. C. S., Lott, M. J., López-Ibarra, G. A., Galván-Magaña, F., Fry, B. 2007. Insight into the Trophic Ecology of Yellowfin Tuna, *Thunnus albacares*, from Compound-Specific Nitrogen Isotope Analysis of Proteinaceous Amino Acids. In Isotopes as Indicators of Ecological Change: Vol. I. doi:10.1016/S1936-7961(07)01012-3

Post, D. M. 2002. Using Stable Isotopes to Estimate Trophic Position: Models, Methods, and Assumptions. Ecology, 83(3), 703. doi:10.2307/3071875

Post, D. M., Layman, C. A., Arrington, D. A., Takimoto, G., Quattrochi, J., Montaña, C. G. 2007. Getting to the fat of the matter: models, methods and assumptions for dealing with lipids in stable isotope analyses. Oecologia, 152(1), 179–189. doi:10.1007/s00442-006-0630-x

Potier, M., Marsac, F., Cherel, Y., Lucas, V., Sabatié, R., Maury, O., Ménard, F. 2007. Forage fauna in the diet of three large pelagic fishes (lancetfish, swordfish and yellowfin tuna) in the western equatorial Indian Ocean. Fisheries Research, 83(1), 60–72. doi:10.1016/j.fishres.2006.08.020

Quezada-Romegialli, C., Jackson, A. L., Hayden, B., Kahilainen, K. K., Lopes, C., Harrod, C. 2018. tRophicPosition, an r package for the Bayesian estimation of trophic position from consumer stable isotope ratios. Methods in Ecology and Evolution, 9(6), 1592–1599. doi:10.1111/2041-210X.13009

Rabalais, N. N., Turner, R. E., Dortch, Q., Justic, D., Bierman Jr., V. J., Wiseman Jr., W. J. 2002. Nutrient-enhanced productivity in the northern Gulf of Mexico: Past, present and future. Hydrobiologia, 475(3), 39–63. doi:10.1023/A:1020388503274

Rabalais, N. N., Turner, R. E., Wiseman, W. J. 2002. Gulf of Mexico hypoxia, a.k.a. "The dead zone". Annual Review of Ecology and Systematics, 33, 235–263. doi:10.1146/annurev.ecolsys.33.010802.150513

Reyes-Mendoza, O., Mariño-Tapia, I., Herrera-Silveira, J., Ruiz-Martínez, G., Enriquez, C., Largier, J. L. 2016. The Effects of Wind on Upwelling off Cabo Catoche. Journal of Coastal Research, 319, 638–650. doi:10.2112/JCOASTRES-D-15-00043.1

Richards, W. J. 1969. An hypothesis on yelllowfin tuna migrations in the eastern Gulf of Guinea. Océanographie, VII(3), 3–7.

Richards, W. J. (Ed.). (2005). Early stages of Atlantic fishes: an identification guide for the western central north Atlantic, Two Volume Set. CRC Press.

Richardson, A. J., Downes, K. J., Nolan, E. T., Brickle, P., Brown, J., Weber, N., Weber, S. B. 2018. Residency and reproductive status of yellowfin tuna in a proposed large-scale pelagic marine protected area. Aquatic Conservation: Marine and Freshwater Ecosystems, 28(6), 1308–1316. doi:10.1002/aqc.2936

Rooker, J. R., Dance, M. A., Wells, R. J. D., Ajemian, M. J., Block, B. A., Castleton, M. R., Drymon, J. M., Falterman, B. J., Franks, J. S., Hammerschlag, N., Hendon, J. M., Hoffmayer, E. R., Kraus, R. T., Mckinney, J. A., Secor, D. H., Stunz, G. W. 2019. Population connectivity of pelagic megafauna in the Cuba-Mexico- United States triangle. (December 2018), 1–13. doi:10.1038/s41598-018-38144-8

Rooker, J. R., Turner, J. P., Holt, S. A. 2006. Trophic ecology of Sargassum -associated fishes in the Gulf of Mexico determined from stable isotopes and fatty acids. 313, 249–259. doi:10.3354/meps313249

Sandel, V., Kiko, R., Brandt, P., Dengler, M., Stemmann, L., Vandromme, P., Sommer, U., Hauss, H. 2015. Nitrogen Fuelling of the Pelagic Food Web of the Tropical Atlantic. PLOS ONE, 10(6), e0131258. doi:10.1371/journal.pone.0131258

Savage, C. 2017. Tracing the Influence of Sewage Nitrogen in a Coastal Ecosystem Using Stable Nitrogen Isotopes. Ambio, 34(2), 145–150.

Schaefer, K. M., Fuller, D. W., Block, B. A. 2007. Movements, behavior, and habitat utilization of yellowfin tuna (*Thunnus albacares*) in the northeastern Pacific Ocean, ascertained through archival tag data. Marine Biology, 152(3), 503–525. doi:10.1007/s00227-007-0689-x

Schaefer, K. M. 1998. Reproductive biology of yellowfin tuna *(Thunnus alabacare*s) in the eastern Pacific Ocean. In: Inter-American Tropical Tuna Commission Bulletin (Vol. 21).

Schaefer, K.M. 2001. Reproductive biology of tunas. In: Block B., Stevens. (Eds). Tuna: Physiology, ecology and evolution. Academic Press Monterey pp. 225-262

Seki, M. P., Polovina, J. J., Brainard, R. E., Bidigare, R. R., Leonard, C. L., Foley, D. G. 2001. Biological enhancement at cyclonic eddies tracked with GOES thermal imagery in Hawaiian waters. Geophysical Research Letters, 28(8), 1583–1586. doi:10.1029/2000GL012439

Seminoff, J. A., Benson, S. R., Arthur, K. E., Eguchi, T., Dutton, P. H., Tapilatu, R. F., Popp, B. N. 2012. Stable Isotope Tracking of Endangered Sea Turtles: Validation with Satellite Telemetry and δ15N Analysis of Amino Acids. PLoS ONE, 7(5), e37403. doi:10.1371/journal.pone.0037403

Sibert, J., Hampton, J., Kleiber, P., Maunder, M. 2006. Biomass, Size, and Trophic Status of Top Predators in the Pacific Ocean. Science, 314(5806), 1773–1776. doi:10.1126/science.1135347

Sigman, D. M., Casciotti, K. L. 2001. Nitrogen Isotopes in the Ocean. In Encyclopedia of Ocean Sciences. doi:10.1006/rwos.2001.0172

Sosa-nishizaki, O., Ramirez-Mendoza, Z., Fajardo-Yamamoto, A. 2017. Reporte del primer crucero de marcaje de atún aleta amarilla (*Thunnus albacares*) y resultados preliminares de los datos de distribución vertical y horizontal. Ensenada.1-16

Sulzman, E. W. 2007. Chapter 1: Stable isotope chemistry and measurement: a primer. In R. Michener & K. Lajtha (Eds.), Ecological methods and concepts series (Second). doi:10.1899/0887-3593-028.002.0516

Sturges, W., Leben, R. 2000. Frequency of ring separations from the Loop Current in the Gulf of Mexico: A revised estimate. Journal of Physical Oceanography, 30(7), 1814–1819. doi:10.1175/1520-0485(2000)030<1814:FORSFT>2.0.CO;2

Sweeting, C. J., Jennings, S., Polunin, N. V. C. 2005. Variance in isotopic signatures as a descriptor of tissue turnover and degree of omnivory. 777–784. doi:10.1111/j.1365-2435.2005.01019.x

Szpak, P. 2014. Complexities of Nitrogen Isotope Biogeochemistry in Plant-Soil Systems : Complexities of nitrogen isotope biogeochemistry in plant-soil systems : implications for the study of ancient agricultural and animal management practices. (June). doi:10.3389/fpls.2014.00288

Teo, S. L. H., Block, B. A. 2010. Comparative Influence of Ocean Conditions on Yellowfin and Atlantic Bluefin Tuna Catch from Longlines in the Gulf of Mexico. PLoS ONE, 5(5), e10756. doi:10.1371/journal.pone.0010756

Tussadiah, A., Pranowo, W. S., Syamsuddin, M. L., Riyantini, I., Nugraha, B., Novianto, D. 2018. Characteristic of eddies kinetic energy associated with yellowfin tuna in southern Java Indian Ocean. IOP Conference Series: Earth and Environmental Science, 176(1), 012004. doi:10.1088/1755-1315/176/1/012004

Vander Zanden, J., Rasmussen Joseph. 1999. Primary consumer δ13C and δ15N and the trophic of aquatic consumers. Ecology, 80(4), 1395–1404. doi:10.1890/0012-9658(1999)080[1395:PCCANA]2.0.CO;2

Vander Zanden, M. J. Vander, Clayton, M. K., Moody, E. K., Solomon, C. T., Weidel, B. C. 2015. Stable Isotope Turnover and Half-Life in Animal Tissues : A Literature Synthesis. PLoS ONE, 10(1), 1–16. doi:10.1371/journal.pone.0116182

Vanderklift, M. A., Ponsard, S. 2003. Sources of variation in consumer-diet δ15N enrichment: A meta-analysis. Oecologia, 136(2), 169–182. doi:10.1007/s00442-003-1270-z

Varela, J. L., Intriago, K. M., Flores, J. C., Lucas-Pilozo, C. R. 2017. Feeding habits of juvenile yellowfin tuna (*Thunnus albacares*) in Ecuadorian waters assessed from stomach content and stable isotope analysis. Fisheries Research, 194(May), 89–98. doi:10.1016/j.fishres.2017.05.017

Vaske Jr, T., Castello, J. P. 1998. Conteúdo estomacal da albacora-laje, *Thunnus albacares*, durante o inverno e primavera no sul do Brasil. Revista Brasileira de Biologia, 58(4), 639–647. doi:10.1590/S0034-71081998000400011

Vaske Jr, T., Vooren, C. M., Lessa, R. P. 2003. Feeding strategy of yellowfin tuna (*Thunnus albacare*s), and wahoo (*Acanthocybium solandri*) in the Saint Peter and Saint Paul Archipelago, Brazil. Boletim Do Instituto De Pesca, 29(2), 173–181.

Vokhshoori, N. L., McCarthy, M. D. 2014. Compound-Specific δ15N Amino Acid Measurements in Littoral Mussels in the California Upwelling Ecosystem: A New Approach to Generating Baseline δ15N Isoscapes for Coastal Ecosystems. PLoS ONE, 9(6), e98087. doi:10.1371/journal.pone.0098087

Walli, A., Teo, S. L. H., Boustany, A., Farwell, C. J., Williams, T., Dewar, H., Prince, E., Block, B. A. 2009. Seasonal movements, aggregations and diving behavior of Atlantic bluefin tuna (*Thunnus thynnus*) revealed with archival tags. PLoS ONE, 4(7). doi:10.1371/journal.pone.0006151

Watanabe, Y. Y., Goldman, K. J., Caselle, J. E., Chapman, D. D., Papastamatiou, Y. P. 2015. Comparative analyses of animal-tracking data reveal ecological significance of endothermy in fishes. Proceedings of the National Academy of Sciences, 112(19), 6104–6109. doi:10.1073/pnas.1500316112

Wells, R. J. D., Rooker, J. R., Quigg, A., Wissel, B. 2017. Influence of mesoscale oceanographic features on pelagic food webs in the Gulf of Mexico. Marine Biology, 164(4), 1–11. doi:10.1007/s00227-017-3122-0

Weng, J.-S., Lee, M.-A., Liu, K.-M., Hsu, M.-S., Hung, M.-K., Wu, L.-J. 2015. Feeding Ecology of Juvenile Yellowfin Tuna from Waters Southwest of Taiwan Inferred from Stomach Contents and Stable Isotope Analysis. Marine and Coastal Fisheries, 7(1), 537–548. doi:10.1080/19425120.2015.1094157

Weng, K. C., Stokesbury, M. J. W., Boustany, A. M., Seitz, A. C., Teo, S. L. H., Miller, S. K., Block, B. A. 2009. Habitat and behaviour of yellowfin tuna *Thunnus albacares* in the Gulf of Mexico determined using pop-up satellite archival tags. Journal of Fish Biology, 74(7), 1434–1449. doi:10.1111/j.1095-8649.2009.02209.x

Yáñez-Arancibia, A., Day, J. W., Currie-Alder, B. 2009. Functioning of the Grijalva-Usumacinta River Delta, Mexico: Challenges for Coastal Management. Ocean Yearbook Online, 23(1), 473–501. doi:10.1163/22116001-90000205

Yarnes, C. T., Herszage, J. 2017. The relative influence of derivatization and normalization procedures on the compound-specific stable isotope analysis of nitrogen in amino acids. Rapid Communications in Mass Spectrometry, 31(8), 693–704. doi:10.1002/rcm.7832

Young, J. W., Hunt, B. P. V., Cook, T. R., Llopiz, J. K., Hazen, E. L., Pethybridge, H. R., Ceccarelli, D., Lorrain, A., Olson, R. J., Allain, V., Menkes, C., Patterson, T., Nicol, S., Lehodey, P., Kloser, R. J., Arrizabalaga, H., Anela Choy, C. 2015. The trophodynamics of marine top predators: Current knowledge, recent advances and challenges. Deep Sea Research Part II: Topical Studies in Oceanography, 113(March), 170–187. doi:10.1016/j.dsr2.2014.05.015

Zavala-Hidalgo, J., Gallegos-García, A., Martínez-López, B., Morey, S. L., O'Brien, J. J. 2006. Seasonal upwelling on the Western and Southern Shelves of the Gulf of Mexico. Ocean Dynamics, 2006, 56(3–4), pp. 333–338. doi:10.1007/s10236-006-0072-3

Supplementary material

Table 4. Individual ID, collection year, curved fork length in centimeters, $\delta^{13}C$ values and $\delta^{15}N$ values in *per mil (‰)*, and C:N for white muscle and liver of yellowfin tuna caught in southern Gulf of Mexico.

ID	Collection Year	CFL	Muscle			Liver		
			$\delta^{13}C$	$\delta^{15}N$	C:N	$\delta^{13}C$	$\delta^{15}N$	C:N
1	2017	123	-18.8	10.1	3.77	-19.6	7.1	4.22
2	2017	125	-18.7	9.4	3.65	-19.1	7.1	3.81
3	2017	128	-17.6	9.9	3.19	-19.1	8.0	3.98
4	2017	129	-19.5	10.4	4.21	-19.7	8.1	4.51
5	2017	130	-17.6	9.5	3.20	-18.7	7.8	3.82
6	2017	131	-19.0	10.0	4.02	-18.9	7.8	3.94
7	2017	131	-18.8	10.1	3.75	-19.4	7.7	4.12
8	2017	132	-17.5	9.3	3.23	-18.9	7.8	4.01
9	2017	139	-18.2	10.4	3.37	-20.0	7.7	4.54
10	2017	140	-18.7	10.3	3.70	-19.2	8.2	4.09
11	2017	143	-18.5	9.8	3.64	-19.1	8.0	4.07
12	2017	145	-17.1	9.8	3.12	-18.9	7.4	3.82
13	2017	146	-20.1	10.9	4.44	-19.2	8.9	4.26
14	2017	146	-18.5	10.2	3.64	-20.1	8.0	4.73
15	2018	140	-17.8	10.7	3.39	-18.2	8.2	3.87
16	2018	141	-18.1	10.5	3.34	-19.3	8.6	4.49
17	2018	140	-18.5	10.3	3.60	-19.7	8.0	4.71
18	2018	136	-18.0	10.0	3.31	-18.8	7.4	4.11
19	2018	139	-17.5	10.9	3.18	-19.2	8.3	4.85
20	2018	131	-17.6	11.0	3.23	-18.6	7.8	3.97
21	2018	137	-18.1	10.4	3.27	-18.5	7.5	3.91
22	2018	139	-17.5	9.6	3.29	-18.6	6.2	4.05
23	2018	133	-17.4	10.9	3.21	-18.1	8.0	3.85
24	2018	137	-17.9	9.1	3.34	-18.8	6.5	4.04
25	2018	141	-18.6	9.6	3.60	-18.6	7.0	4.00
26	2018	146	-19.3	10.5	3.21	-18.9	7.9	4.29
27	2018	144	-17.6	12.7	3.93	-18.2	9.2	3.92
28	2018	132	-17.7	10.1	3.30	-18.6	8.1	4.30
29	2018	146	-18.7	10.1	3.71	-18.6	8.5	4.09
30	2018	134	-17.1	9.1	3.20	-17.9	7.7	3.86
31	2018	145	-17.9	9.3	3.37	-18.2	8.3	4.00
32	2018	150	-18.0	11.9	3.43	-18.5	8.2	4.10
33	2018	132	-18.3	9.7	3.44	-18.6	7.8	4.04
34	2018	136	-17.6	9.2	3.27	-18.1	8.0	3.86
35	2018	138	-17.8	10.0	3.15	-18.5	7.8	3.86
36	2018	145	-17.3	9.1	3.27	-18.4	7.5	3.97
37	2018	135	-17.6	9.7	3.19	-18.8	7.2	4.21
38	2018	146	-17.6	10.0	3.17	-18.9	7.5	4.38

39	2018	133	-18.0	9.1	3.47	-18.6	7.9	4.28
40	2018	131	-17.2	9.1	3.12	-18.6	6.9	3.99
41	2018	139	-17.7	10.0	3.14	-18.3	7.9	4.06
42	2018	144	-17.8	9.5	3.31	-18.6	7.0	3.98
43	2018	137	-18.1	9.6	3.47	-19.1	8.1	4.79
44	2018	152	-17.4	9.5	3.32	-18.4	7.4	4.40
45	2018	146	-17.6	10.1	3.25	-18.7	7.9	4.43
46	2018	146	-17.6	10.0	3.16	-18.9	6.9	4.16
47	2018	143	-17.5	10.0	3.18	-18.6	8.1	4.14
48	2018	135	-17.3	10.0	3.20	-18.6	7.0	4.04
49	2018	128	-17.8	9.5	3.35	-18.3	7.7	3.96
50	2018	142	-17.5	10.1	3.23	-18.3	7.8	4.16
51	2018	139	-17.6	9.5	3.19	-18.5	8.0	4.06
52	2018	146	-18.4	10.0	3.56	-20.0	7.3	5.23
53	2018	130	-17.8	9.5	3.25	-18.6	8.1	4.23
54	2018	131	-17.7	9.7	3.30	-19.0	7.3	4.08
55	2018	138	-17.7	9.9	3.21	-18.7	7.1	3.99
56	2018	154	-17.8	10.0	3.36	-18.6	7.9	4.25
57	2018	134	-17.4	9.4	3.23	-18.7	7.6	4.39
58	2018	135.5	-17.6	9.8	3.22	-18.2	7.6	4.17
59	2018	138	-17.5	10.7	3.26	-19.1	7.2	4.29
60	2018	137	-18.1	9.8	3.42	-19.5	7.3	4.69
61	2018	146	-18.6	10.2	3.75	-18.9	8.2	4.17
62	2018	135	-17.8	9.6	3.32	-18.7	7.1	4.19
63	2018	152	-17.8	10.3	3.28	-19.1	8.2	4.39
64	2018	145	-17.8	12.4	3.32	-18.3	9.1	4.06
65	2018	160	-17.4	10.2	3.17	-19.2	7.0	4.57
66	2018	144	-17.8	9.9	3.28	-18.5	8.1	4.32
67	2018	154	-17.9	12.9	3.34	-17.9	10.9	3.73
68	2018	145	-17.5	9.9	3.29	-18.5	7.9	4.09
69	2018	134	-17.3	9.6	3.22	-18.6	7.5	4.19
70	2018	138	-17.9	9.7	3.31	-18.9	7.6	4.30
71	2018	152	-17.5	9.9	3.29	-18.2	7.5	4.22
72	2018	145	-18.0	10.3	3.26	-19.1	7.4	4.47

Table 5. Cruise, stations, coordinates in decimal degrees, and $\delta^{13}C$ and $\delta^{15}N$ values of zooplankton (fraction size 335-1000 µm) are shown. *Correspond to stations used as northern Gulf of Mexico (GM), †correspond to stations used as central-southern GM.

Cruise	Station ID	Latitude	Longitude	$\delta^{13}C$	$\delta^{15}N$
GOMECC-03	E1†	26.004	-86.004	-19.1	1.2
GOMECC-03	E2†	26.656	-85.004	-20.5	2.4
GOMECC-03	E3*	27.330	-84.002	-21.7	4.8
GOMECC-03	E4*	27.775	-83.332	-20.5	4.9
GOMECC-03	E5*	29.378	-85.511	-21.1	6.4
GOMECC-03	E6*	29.027	-85.790	-21.0	7.9
GOMECC-03	E8*	28.000	-86.635	-20.5	3.1
GOMECC-03	E9*	27.581	-90.004	-20.3	3.5
GOMECC-03	E10*	27.923	-89.999	-19.9	3.3
GOMECC-03	E11*	28.498	-90.001	-21.1	8.9
GOMECC-03	E12*	28.937	-90.123	-22.7	11.6
GOMECC-03	E13*	27.813	-93.840	-22.0	7.2
GOMECC-03	E14*	27.809	-93.840	-21.7	7.4
GOMECC-03	E15*	27.815	-93.848	-22.3	7.3
GOMECC-03	E16*	27.813	-93.840	-22.5	7.2
GOMECC-03	E17*	28.090	-95.001	-20.1	5.3
GOMECC-03	E18*	28.335	-94.999	-21.8	8.4
GOMECC-03	E19*	28.669	-94.997	-22.7	9.4
GOMECC-03	E20*	29.002	-94.999	-20.2	11.6
GOMECC-03	E21*	25.878	-96.802	-21.9	4.7
GOMECC-03	E22†	25.880	-96.323	-20.0	1.7
GOMECC-03	E23†	25.881	-95.830	-19.4	2.0
GOMECC-03	E24†	25.878	-94.672	-19.6	2.0
GOMECC-03	E25†	22.274	-97.546	-21.4	3.2
GOMECC-03	E26†	22.269	-97.358	-20.0	2.6
GOMECC-03	E27†	22.267	-96.763	-20.4	1.7
GOMECC-03	E28†	22.268	-94.993	-20.6	2.3
GOMECC-03	E29†	25.046	-88.011	-19.6	2.2
GOMECC-03	E30†	24.394	-87.990	-21.1	2.2
GOMECC-03	E31†	23.772	-87.997	-21.3	2.7
GOMECC-03	E32†	21.509	-95.602	-19.2	4.0
GOMECC-03	E33†	21.450	-91.564	-19.1	4.3
GOMECC-03	E34†	21.736	-92.315	-20.9	3.3
GOMECC-03	E35†	21.502	-92.541	-20.6	3.2
GOMECC-03	E36†	20.735	-94.750	-20.1	3.2
GOMECC-03	E37†	20.019	-93.762	-19.9	4.1
GOMECC-03	E38†	19.173	-93.299	-21.9	4.5
GOMECC-03	E39†	18.834	-93.065	-21.0	5.2
GOMECC-03	E40†	21.590	-86.497	-19.0	5.0
GOMECC-03	E41†	21.636	-86.232	-19.6	3.3
GOMECC-03	E43	21.833	-84.982	-19.9	1.4

GOMECC-03	E44	23.268	-80.616	-19.4	2.3
GOMECC-03	E45	23.785	-80.617	-20.4	1.7
GOMECC-03	E46b	24.338	-80.578	-19.3	2.2
GOMECC-03	E47	24.745	-80.619	-14.8	3.8
GOMECC-03	E48	26.986	-80.004	-17.8	3.9
GOMECC-03	E49	27.006	-79.875	-20.5	3.4
GOMECC-03	E50	26.988	-79.610	-20.2	3.4
GOMECC-03	E51	26.998	-79.196	-19.0	2.4
XIXIMI-06	A1†	24.881	-95.515	-20.3	1.6
XIXIMI-06	A2†	24.883	-94.985	-20.5	1.6
XIXIMI-06	A10†	24.937	-87.068	-19.2	1.5
XIXIMI-06	B11†	24.007	-96.012	-20.5	1.6
XIXIMI-06	B12†	23.996	-95.086	-21.1	1.6
XIXIMI-06	B13†	23.976	-93.711	-20.3	2.2
XIXIMI-06	B14†	24.056	-92.318	-17.3	1.6
XIXIMI-06	B15†	23.992	-90.995	-18.7	2.5
XIXIMI-06	B17†	24.010	-89.008	-20.4	2.7
XIXIMI-06	B18†	24.021	-86.836	-20.2	1.8
XIXIMI-06	C21†	22.999	-95.500	-20.2	0.9
XIXIMI-06	C22†	23.006	-94.500	-20.7	2.2
XIXIMI-06	C23†	22.977	-93.024	-20.7	1.6
XIXIMI-06	C24†	22.512	-92.008	-19.8	1.6
XIXIMI-06	C25†	22.997	-91.021	-19.6	3.1
XIXIMI-06	D26†	22.020	-97.147	-20.1	2.4
XIXIMI-06	D27†	22.000	-96.001	-19.3	2.1
XIXIMI-06	D28†	22.004	-95.010	-19.7	2.5
XIXIMI-06	D29†	22.009	-94.026	-20.4	3.6
XIXIMI-06	D30†	21.998	-93.013	-19.7	2.7
XIXIMI-06	E32†	22.540	-88.001	-20.3	2.6
XIXIMI-06	E33†	21.496	-94.502	-20.2	2.1
XIXIMI-06	E35†	21.995	-92.913	-21.6	3.2
XIXIMI-06	F37†	21.006	-95.000	-19.9	2.1
XIXIMI-06	F38†	21.008	-93.997	-20.2	3.2
XIXIMI-06	F39†	21.003	-92.990	-20.7	3.4
XIXIMI-06	G40†	20.503	-96.007	-20.8	2.9
XIXIMI-06	G42†	20.512	-94.502	-21.1	3.2
XIXIMI-06	G43†	20.511	-93.510	-20.0	3.9
XIXIMI-06	G44†	20.517	-92.500	-20.7	2.9
XIXIMI-06	H45a†	19.989	-95.626	-20.7	3.2
XIXIMI-06	H45b†	19.989	-95.626	-21.1	3.4
XIXIMI-06	H46x†	20.002	-94.998	-20.4	3.1
XIXIMI-06	H46y†	20.001	-93.996	-20.0	3.6
XIXIMI-06	H48†	20.012	-93.011	-21.3	5.5
XIXIMI-06	J49†	19.503	-94.999	-20.3	3.1
XIXIMI-06	Y2a†	21.602	-86.348	-19.5	2.7

XIXIMI-06	Y2b†	21.610	-86.356	-19.6	2.7
XIXIMI-06	Y3a†	21.662	-86.245	-18.7	2.7
XIXIMI-06	Y3b†	21.677	-86.223	-19.5	3.0
XIXIMI-06	Y6a†	21.676	-86.059	-19.5	2.4
XIXIMI-06	Y6b†	21.695	-86.055	-20.3	2.1
XIXIMI-06	Y7a†	21.718	-85.950	-19.9	2.4
XIXIMI-06	Y7b†	21.717	-85.943	-20.1	2.1

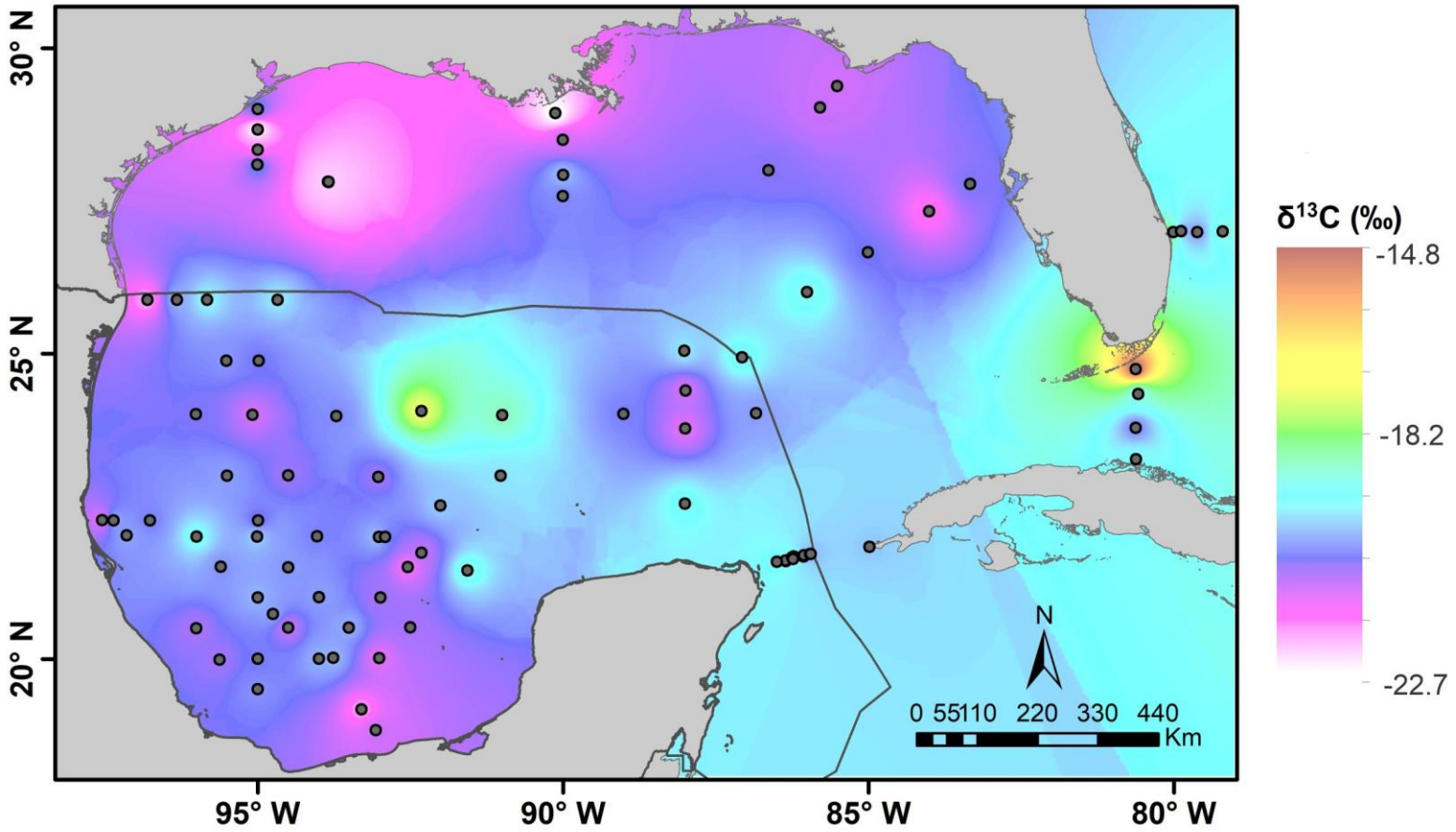

Figure 14. Gulf of Mexico (GM) zooplankton-based $\delta^{13}C$ isoscape generated with IDW interpolation of zooplankton size 335-1000 µm.

Table 6. Average of the standard deviations calculated from the duplicate measurements of CSIA-AA made on each sample (n = 2) analyzed in this study, except for samples liver YFT ID 35, 41, muscle YFT ID 11, 47, and GOMECC station 11 (n=3) and sample muscle YFT ID 19 (n=4) which had more than two injections.

Component	Zooplankton	Liver	Muscle
Ala	0.4	0.4	0.4
Aspartic Acid + Asparagine	0.3	0.3	0.4
Glutamic Acid + Glutamine	0.3	0.5	0.4
Glycine	0.4	0.3	0.4
Histidine	0.8	0.6	0.9
Hydroxyproline	0.9	0.5	n.m.
Isoleucine	0.5	0.7	0.8
Leucine	0.2	0.3	0.3
Lysine	0.5	0.5	0.6
Methionine	0.4	0.6	0.7
Phenylalanine	0.4	0.5	0.5
Proline	0.3	0.4	0.6
Serine	0.4	0.4	0.6
Threonine	0.3	0.4	0.4
Tyrosine	0.5	0.6	0.7
Valine	0.4	0.4	0.4

Table 7. Collection year, YFT ID number, muscle $\delta^{15}N$ values (‰) of bulk, source amino acids (Lys, Met, Phe), trophic amino acids (Ala, Asx, Glu, Leu, Pro, and Val) and "Metabolic" amino acids (Ile, Gly, Ser, Thr, His, Hyp) (O'Connell 2017).

Year	YFT ID	Bulk	Lys	Met	Phe	Ala	Asx	Glu	Leu	Pro	Val	Ile	His	Gly	Ser	Thr	Tyr	Hyp
2017	1	10.1	5.0	10.1	6.2	27.2	28.4	25.9	25.3	18.9	26.5	n.m.	n.m.	-5.2	1.7	-32.2	4.0	n.m.
2017	2	9.4	2.9	9.5	5.4	23.1	27.8	25.9	24.8	20.6	25.1	n.m.	n.m.	-6.9	1.2	-32.9	1.8	n.m.
2017	3	9.9	4.2	9.9	5.0	25.6	28.4	26.8	25.2	19.6	26.6	n.m.	n.m.	-5.6	1.5	-32.2	2.1	n.m.
2017	4	10.4	4.1	10.0	6.7	25.2	28.9	27.1	25.5	21.9	27.3	n.m.	n.m.	-6.2	3.3	-31.4	1.8	n.m.
2017	5	9.5	3.2	10.4	7.0	24.8	27.6	25.7	23.5	18.3	25.4	n.m.	n.m.	-6.2	1.9	-31.3	0.5	n.m.
2017	6	10.0	3.8	10.2	5.8	25.5	28.2	26.2	24.6	19.5	26.8	n.m.	n.m.	-6.4	1.5	-32.8	1.2	n.m.
2017	7	10.1	3.7	10.3	4.4	27.1	28.3	26.1	24.9	20.8	26.5	n.m.	n.m.	-7.0	1.0	-33.9	1.8	n.m.
2017	8	9.3	2.9	9.2	6.6	21.0	27.6	25.7	25.1	21.1	25.5	n.m.	n.m.	-8.5	1.1	-33.6	0.1	n.m.
2017	9	10.4	4.5	10.9	4.4	25.9	28.6	26.3	25.3	22.2	26.6	n.m.	n.m.	-6.8	1.3	-34.8	4.9	n.m.
2017	10	10.3	4.5	11.2	6.7	24.5	29.1	27.0	25.1	20.1	26.0	n.m.	n.m.	-7.0	1.5	-33.4	1.9	n.m.
2017	11	9.8	3.7	9.1	5.5	25.8	27.6	26.6	25.5	20.5	26.8	n.m.	n.m.	-6.6	2.4	-33.2	1.0	n.m.
2017	12	9.8	3.4	10.6	8.7	24.1	27.9	25.9	24.9	17.4	24.9	n.m.	n.m.	-8.8	1.3	-32.1	0.4	n.m.
2017	13	10.9	4.5	11.0	6.2	24.8	29.2	27.0	25.9	20.7	26.7	n.m.	n.m.	-6.5	1.1	-33.6	2.8	n.m.
2017	14	10.2	4.3	9.2	5.4	24.5	29.0	26.7	25.1	20.8	25.9	n.m.	n.m.	-7.1	1.0	-34.3	1.4	n.m.
2018	18	10.0	3.4	10.6	6.2	22.7	27.7	25.8	25.0	21.3	26.8	25.9	4.5	-6.0	0.2	-32.5	11.7	n.m.
2018	24	9.1	2.5	10.6	5.7	22.4	27.0	24.7	24.5	22.4	25.5	27.4	2.0	-7.3	-1.2	-33.5	9.0	n.m.
2018	27	12.7	5.4	12.3	9.0	25.9	30.2	28.3	27.7	24.5	29.1	27.5	7.6	-0.9	3.6	-27.8	10.3	n.m.
2018	28	10.1	2.4	11.3	8.1	23.8	28.7	26.8	26.6	24.7	28.5	27.6	3.9	-8.2	-1.8	-36.9	11.0	n.m.
2018	31	9.3	2.3	9.6	6.9	22.3	27.4	25.7	25.0	20.1	26.6	26.7	3.3	-7.4	-1.1	-34.2	10.2	26.7
2018	32	11.9	3.0	10.9	5.6	25.0	30.3	26.7	26.7	23.0	28.4	30.0	7.5	-4.3	-1.4	-33.3	8.5	n.m.
2018	33	9.7	2.9	10.6	6.7	22.9	27.2	25.7	25.4	22.6	26.6	28.7	3.4	-6.3	-0.6	-32.8	8.5	n.m.
2018	36	9.1	2.8	10.9	6.4	22.4	26.6	24.2	24.7	21.9	26.0	25.9	4.3	-8.0	-2.1	-37.8	11.0	n.m.
2018	37	9.7	3.4	9.9	5.4	22.5	27.0	25.2	24.9	22.2	26.4	25.1	4.2	-7.6	-1.4	-33.8	10.3	n.m.

2018	38	10.0	3.4	10.1	5.3	22.4	26.6	25.0	25.1	21.7	26.8	26.9	5.2	-6.7	-0.7	-34.7	9.5	n.m.
2018	44	9.5	2.9	10.8	6.8	22.4	27.8	25.1	25.4	20.5	26.7	25.6	3.5	-7.7	-1.8	-36.7	8.5	n.m.
2018	45	10.1	2.5	9.0	4.4	21.3	26.8	24.0	24.3	21.1	24.5	28.5	7.7	-7.3	-2.5	-36.1	10.2	n.m.
2018	48	10.0	1.8	10.0	7.8	22.1	28.2	25.3	26.1	19.5	26.8	31.1	4.0	-8.8	-2.7	-36.1	10.6	n.m.
2018	51	9.5	1.5	9.5	7.4	20.7	27.1	24.7	25.0	18.2	25.8	29.6	3.9	-8.4	-2.1	-33.2	7.9	n.m.
2018	54	9.7	1.8	9.1	4.7	19.4	25.7	23.6	24.2	19.3	24.6	29.1	4.3	-8.6	-2.0	-33.4	8.5	n.m.
2018	60	9.8	2.5	14.0	7.4	21.5	28.9	25.5	25.3	20.5	26.6	29.7	4.9	-7.9	-2.1	-34.3	9.5	n.m.
2018	64	12.4	4.3	12.3	9.1	23.9	29.9	26.2	27.2	19.7	27.9	32.0	7.5	-4.0	0.8	-29.4	12.8	n.m.
2018	66	9.9	2.8	8.5	5.3	21.9	26.9	23.1	24.4	21.1	25.2	28.6	8.1	-7.4	-2.4	-32.7	9.5	n.m.
2018	67	12.9	5.0	12.6	7.7	25.8	30.9	28.6	27.8	23.5	28.9	27.5	8.4	-0.8	3.7	-30.0	12.4	n.m.
2018	69	9.6	1.3	10.0	5.6	20.7	26.5	23.4	24.1	18.1	24.6	28.5	4.1	-9.1	-3.8	-34.9	9.4	n.m.
2018	70	9.7	0.9	9.9	7.2	20.9	28.2	24.4	24.9	21.1	25.5	29.7	4.7	-9.4	-3.3	-33.8	9.6	n.m.
2018	72	10.3	1.5	11.3	4.0	20.9	26.8	23.7	24.3	19.5	25.4	28.6	7.6	-8.5	-3.8	-35.6	9.4	n.m.

Table 8. Collection year, YFT ID number, liver $\delta^{15}N$ values (‰) of bulk, source amino acids (Lys, Met, Phe), trophic amino acids (Ala, Asx, Glu, Leu, Pro, and Val) and "Metabolic" amino acids (Ile, Gly, Ser, Thr, His, Hyp) (O'Connell 2017).

Year	YFT ID	Bulk	Lys	Met	Phe	Ala	Asx	Glu	Leu	Pro	Val	Ile	His	Gly	Ser	Thr	Tyr	Hyp
2017	1	7.1	2.1	8.0	5.3	16.6	16.0	18.9	19.5	16.5	22.7	n.m.	n.m.	-1.4	2.1	-32.3	4.8	n.m.
2017	2	7.1	1.4	7.2	4.0	18.9	16.5	19.8	20.8	18.5	23.3	n.m.	n.m.	-2.6	1.5	-32.5	4.7	n.m.
2017	3	8.0	2.2	8.1	4.5	16.9	17.1	19.6	20.1	19.9	22.6	n.m.	n.m.	-1.3	2.6	-33.6	5.8	n.m.
2017	4	8.1	3.0	8.9	5.9	17.7	18.4	20.4	21.5	19.4	24.8	n.m.	n.m.	-2.5	1.3	-32.0	6.3	n.m.
2017	5	7.8	2.3	7.2	5.0	19.3	17.4	20.1	20.0	19.4	24.4	n.m.	n.m.	-2.1	1.6	-32.8	4.5	n.m.
2017	6	7.8	3.4	6.6	4.4	19.7	16.2	19.9	20.2	20.6	23.3	n.m.	n.m.	-1.9	0.5	-35.0	4.6	n.m.
2017	7	7.7	2.3	8.3	4.7	18.1	17.2	20.0	20.3	17.8	24.1	n.m.	n.m.	-2.4	1.2	-34.4	5.7	n.m.
2017	8	7.8	0.9	6.1	4.4	19.3	17.5	19.9	20.1	20.1	23.0	n.m.	n.m.	-2.9	0.6	-35.1	4.0	n.m.
2017	9	7.7	2.3	7.9	3.5	18.8	16.1	20.6	20.9	19.5	24.8	n.m.	n.m.	-1.9	1.5	-34.9	4.6	n.m.
2017	10	8.2	2.5	9.6	4.3	19.5	16.9	20.1	20.4	20.8	23.5	n.m.	n.m.	-1.7	1.3	-34.0	4.9	n.m.
2017	11	8.0	2.0	8.1	4.5	18.0	17.7	20.4	20.5	20.6	24.3	n.m.	n.m.	-1.2	2.7	-35.5	5.1	n.m.
2017	12	7.4	2.4	8.4	5.2	20.1	17.3	20.7	21.5	19.5	25.4	n.m.	n.m.	-3.0	0.6	-34.1	4.0	n.m.
2017	13	8.9	3.5	9.6	5.1	20.6	19.7	21.8	22.3	20.7	24.7	n.m.	n.m.	-3.4	0.4	-33.0	5.2	n.m.
2017	14	8.0	2.6	6.7	4.2	18.4	16.7	20.1	20.2	20.2	23.2	n.m.	n.m.	-1.9	1.1	-33.7	3.6	n.m.
2018	18	7.4	4.8	10.1	4.7	17.1	18.1	19.1	22.4	17.4	24.1	23.1	6.6	-3.4	-0.4	-32.0	8.9	n.m.
2018	24	6.5	2.9	8.1	2.9	16.0	14.4	17.4	19.3	17.5	22.2	20.4	4.6	-1.9	-0.3	-34.4	6.7	n.m.
2018	27	9.2	2.2	11.1	5.5	17.1	19.8	20.3	22.8	20.4	25.1	23.5	7.5	0.1	1.3	-34.1	12.1	n.m.
2018	28	8.1	4.9	10.4	6.2	17.0	18.3	19.6	23.0	20.7	25.1	24.1	8.4	-3.7	-1.9	-37.6	9.3	n.m.
2018	31	8.3	4.5	10.7	5.7	17.0	18.9	19.6	22.5	22.5	24.2	23.7	5.1	-2.4	-1.2	-35.4	10.1	19.9
2018	32	8.2	5.2	9.8	4.5	17.0	17.6	19.7	21.9	19.8	24.2	23.2	6.6	-2.7	-1.0	-35.5	9.2	n.m.
2018	33	7.8	1.8	9.4	4.1	18.4	16.2	18.5	20.6	21.2	23.2	20.6	6.4	-1.4	-0.2	-35.9	9.7	n.m.
2018	36	7.5	1.9	9.9	4.8	18.0	19.8	19.6	22.6	17.3	23.8	22.5	4.8	-5.7	-2.7	-34.4	9.9	n.m.
2018	37	7.2	2.4	9.2	3.7	17.0	16.7	18.9	19.8	15.8	22.5	24.6	n.m.	-2.9	0.2	-31.5	9.2	n.m.

2018	38	7.5	2.8	9.5	2.5	16.9	18.1	19.2	21.2	16.5	23.6	21.4	6.0	-2.9	-0.3	-32.9	9.1	n.m.
2018	44	7.4	3.7	9.0	5.1	12.5	18.4	18.7	22.1	22.1	24.2	21.6	4.5	-2.2	-2.3	-37.7	9.8	n.m.
2018	45	7.9	2.1	8.5	3.0	14.2	18.0	18.8	21.6	16.5	22.7	21.0	5.1	-1.9	-1.0	-33.7	8.9	n.m.
2018	48	7.0	2.7	8.1	4.3	13.4	16.7	18.1	21.2	17.2	23.0	21.8	4.5	-1.2	-0.6	-33.2	8.5	n.m.
2018	51	8.0	2.6	9.0	3.5	15.2	18.1	18.5	20.7	18.7	22.8	21.2	5.5	-1.3	-0.3	-33.6	9.5	n.m.
2018	54	7.3	3.1	8.8	3.4	16.9	17.0	18.7	20.7	16.8	22.8	20.9	7.1	0.2	0.1	-32.0	10.2	n.m.
2018	60	8.2	2.2	9.4	3.0	16.6	16.3	17.8	20.1	20.9	22.7	18.9	4.6	0.6	-0.5	-35.0	8.6	n.m.
2018	64	9.1	3.8	10.3	5.0	17.2	17.9	19.2	22.5	20.2	24.3	23.2	6.6	1.2	1.4	-33.2	11.1	n.m.
2018	66	8.1	3.5	9.1	3.8	18.3	19.2	19.5	23.2	20.2	25.1	23.0	4.7	0.7	-0.1	-35.9	9.7	n.m.
2018	67	10.9	3.9	10.9	6.8	20.0	23.4	21.4	25.4	20.1	27.3	25.7	9.8	3.7	2.4	-33.2	13.2	n.m.
2018	69	7.5	3.7	9.2	3.8	17.0	19.1	19.0	22.0	14.8	23.3	21.5	7.5	-2.6	-1.0	-28.9	10.4	n.m.
2018	70	7.6	3.5	8.8	2.9	19.1	17.4	19.4	20.5	18.8	23.0	21.4	5.8	-0.7	-0.5	-33.0	9.9	n.m.
2018	72	7.4	3.6	8.6	1.7	17.2	19.2	19.3	22.2	16.9	23.4	21.0	5.1	-0.7	-0.4	-32.5	7.2	n.m.

Table 9. Stations classified as northern Gulf of Mexico (GM) and central-Southern GM, and outside the Gulf of Mexico (OGM) $\delta^{15}N$ values of zooplankton (fraction size >2000 µm) of source amino acids (Lys, Met, Phe), trophic amino acids (Ala, Asx, Glu, Leu, Pro and Val) and "Metabolic" amino acids (Ile, Gly, Ser, Thr, His, Hyp) (O'Connell 2017).

	Stations	Lys	Met	Phe	Ala	Asx	Glu	Leu	Pro	Val	Ile	Gly	Ser	Thr	Tyr	His	Hyp
Northern GM	E5+E6	5.1	8.3	3.2	19.4	15.8	19.6	17.7	13.4	19.1	18.8	6.0	5.6	-11.8	6.3	5.2	11.0
	E11	6.2	9.4	4.2	17.3	15.7	18.5	16.2	15.3	18.2	18.7	5.5	6.1	-8.5	7.9	7.4	14.3
	E12	10.5	12.1	6.6	21.6	19.4	22.4	19.5	18.3	21.9	21.8	11.0	8.7	-5.3	11.2	10.3	17.6
	E19	6.8	9.8	5.4	20.3	17.6	20.3	18.7	15.4	21.7	20.8	8.0	7.7	-8.9	9.1	8.9	13.7
	E20	10.6	12.8	8.5	22.3	19.8	22.9	21.6	21.6	22.6	21.7	9.8	10.3	-4.6	13.6	9.6	19.8
	E21	5.2	7.1	4.2	15.4	12.9	15.8	13.3	12.1	16.4	15.5	3.0	4.6	-7.4	6.7	4.0	14.2
Central-suothern GM	E22+E23	-0.9	2.4	-0.9	10.4	8.3	11.1	8.0	7.2	10.5	9.4	-0.3	-0.1	-14.5	1.9	-0.3	6.8
	E25+E26	1.0	4.8	-1.6	13.4	9.7	13.5	9.6	9.1	12.1	10.1	1.8	0.7	-14.3	3.4	0.7	n.m.
	A1+2-B11+12	1.1	4.5	-1.1	13.3	10.7	14.0	12.5	11.3	13.9	13.6	-0.1	0.5	-19.6	4.3	1.8	n.m.
	B14+B15	0.4	4.0	-1.6	14.0	11.4	14.5	11.5	11.5	13.4	11.7	0.0	1.4	-19.0	2.3	1.2	n.m.
	B17	0.9	4.8	-0.3	14.8	11.7	15.4	11.9	9.9	13.7	13.6	1.4	1.3	-17.9	2.7	2.1	n.m.
	E32+E33	0.5	3.5	-0.4	13.0	10.8	13.4	11.5	9.5	13.0	13.5	1.6	1.0	-16.4	2.3	-0.2	8.0
	G43	1.4	4.5	-0.7	15.0	11.4	15.1	12.0	9.8	13.7	13.7	0.2	1.1	-17.3	3.4	1.5	n.m.
	G40	0.1	3.3	-2.0	13.2	10.7	13.7	11.2	9.7	13.5	13.3	-0.3	0.2	-17.5	1.2	0.1	11.4
	E34	2.9	6.5	1.9	16.3	13.3	16.0	13.6	12.0	15.9	14.0	4.6	4.2	-11.1	3.7	5.7	10.2
	E38+E39	4.3	7.2	1.3	15.6	13.2	15.7	13.5	12.6	15.2	15.4	5.1	4.3	-11.4	4.9	4.0	12.7
	Y6a+Y6b+Y7b	-0.2	4.1	-0.9	12.5	11.2	14.6	10.9	9.4	12.4	12.3	-0.5	-0.3	-18.4	1.6	3.7	8.0
	Y2a+Y2b+Y3a	1.3	4.2	-1.1	16.8	12.6	16.1	13.5	11.1	14.6	13.9	2.8	1.9	-19.6	2.1	1.3	n.m.
	E43	-0.1	2.2	-0.2	12.4	9.8	13.2	9.2	8.2	11.7	9.3	2.6	0.5	-16.5	3.2	1.5	n.m.
	E45	-0.6	3.9	-1.0	13.7	11.2	14.7	11.6	8.9	13.9	12.3	-2.5	-1.2	-19.4	4.3	0.3	n.m.
OGM	E48+E50	1.3	5.0	0.0	16.1	12.8	17.7	13.7	11.7	15.3	15.5	-2.1	0.9	-20.1	5.1	1.2	n.m.
	E49+E51	1.9	5.1	0.2	14.4	11.9	15.0	11.9	9.9	14.5	12.9	0.6	2.4	-14.4	3.5	3.7	n.m.

Table 10. Pearson's correlation between curved furcal length (CFL) and each trophic position (TP) estimates using five literature derived TEFs using bulk $\delta^{15}N$ analyses (SIA) and two baselines and TP derived from $\delta^{15}N$ values of Glu and Phe (CSIA). References for TEFs and TDFs following order of appearance in *Results*, Table 2. *indicates significant relationship between curved furcal length (CFL) and trophic position (TP).

		CFL	
TEF	Method	Northern GM	Central-southern GM
2.4	TPSIA1	r= 0.35 p=0.003*	r= 0.32 p= 0.005*
2.1	TPSIA2	r= 0.32 p=0.006*	r= 0.34 p= 0.004*
1.9	TPSIA3	r= 0.33 p=0.005*	r= 0.34 p= 0.004*
1.3	TPSIA4	r= 0.34 p= 0.004*	r= 0.34 p= 0.004*
1.1	TPSIA5	r= 0.34 p= 0.003*	r= 0.34 p= 0.003*
7.6	TPCSIA1	r= -0.04 p= 0.801	
6.3	TPCSIA2	r= -0.05 p= 0.792	
5.7	TPCSIA3	r= -0.07 p= 0.679	
4.9	TPCSIA4	r= -0.01 p= 0.565	
4.0	TPCSIA5	r= 0.17 p= 0.317	